

**ORIENTATIONAL ORDERING OF SMALL MOLECULES IN NEMATIC LIQUID
CRYSTALS**

By

Zorana Danilović

B.Sc., The University of Belgrade, 2001

A THESIS SUBMITTED IN PARTIAL FULFILLMENT OF
THE REQUIREMENTS FOR THE DEGREE OF
MASTER OF SCIENCE

in

THE FACULTY OF GRADUATE STUDIES
DEPARTMENT OF CHEMISTRY

We accept this thesis as conformation
to the required standard

THE UNIVERSITY OF BRITISH COLUMBIA

October 2004

© Zorana Danilović, 2004



Library Authorization

In presenting this thesis in partial fulfillment of the requirements for an advanced degree at the University of British Columbia, I agree that the Library shall make it freely available for reference and study. I further agree that permission for extensive copying of this thesis for scholarly purposes may be granted by the head of my department or by his or her representatives. It is understood that copying or publication of this thesis for financial gain shall not be allowed without my written permission.

ZORANA DANKOVIC'

Name of Author (please print)

07/10/2004

Date (dd/mm/yyyy)

Title of Thesis:

ORIENTATIONAL ORDERING OF SMALL MOLECULES
IN NEMATIC LIQUID CRYSTALS

Degree:

MASTER OF SCIENCE

Year:

2004

Department of

CHEMISTRY

The University of British Columbia

Vancouver, BC Canada

Abstract

Orientational ordering in nematic liquid crystal phases arises from the presence of anisotropic intermolecular forces. To date NMR experiments, theory and Monte Carlo simulations indicate the importance of two main contributions to orientational ordering of small solutes in various liquid crystals and liquid crystal mixtures. The first contribution is well defined and involves short-range interactions that depend on the size and the shape of the solute. The second contribution, which accounts for long-range (electrostatic) interactions, is believed to have lesser impact on the molecular ordering. Which of the electrostatic interactions (induction, electric quadrupole or polarization) are most important is still debated. In order to investigate the impact of electrostatic interactions on molecular ordering, small symmetric molecules with the same size and shape, and therefore the same short-range interactions, but different electrostatic properties were dissolved in various liquid crystals and mixtures of liquid crystals.

Second rank orientational order parameters of solutes in various liquid crystal phases are obtained from analysis of high-resolution NMR spectra. For high-spin systems, initial spectral parameters needed to solve very complicated high-resolution spectra are estimated from selective multiple-quantum NMR spectra, collected using a 3D selective MQ-NMR technique. Structural parameters of the solutes are calculated using non-vibrationally corrected nuclear dipolar coupling constants accurately obtained from analysis of high-resolution NMR spectra.

The contribution of the electrostatic interactions to the orientational ordering of small solutes in liquid crystal phases is discussed in terms of different solutes and different types of liquid crystals by comparing experiment with theoretically determined order parameters. Those comparisons seem to suggest that dipoles have the least impact on orientational ordering of small molecules in nematic liquid crystals. Quadrupole contribution results predict opposite signs of the electric field gradient to the one obtained in similar previous studies.

Experiments with zero-electric-field-gradient mixtures ('magic mixture') show no significant contributions of the electrostatic long-range interaction to the orientational mechanism in the special mixture.

The polarizability effect appears strongly dependent on molecular geometry and in this study appears to be an important electrostatic mechanism of orientation.

Contents

Abstract	ii
Contents	iii
List of Tables	v
List of Figures	vi
List of Abbreviations	vii
Acknowledgement	viii
Dedication	ix
1 Introduction	1
1.1 Liquid Crystals	1
1.2 Nematic Liquid Crystals	2
1.3 Orientational Ordering and Intermolecular Forces in Nematic Liquid Crystals	3
1.4 Orientational Distribution Function and Order Parameter	4
1.5 Orientational Ordering from Experiments	6
1.5.1 NMR Spectra of Oriented Molecules	7
1.5.2 Solutes as Probes of Orientational Order and Intermolecular Forces	9
1.5.3 Multiple-Quantum NMR	10
1.6 Orientational Ordering from Theoretical Calculation	12
1.6.1 Statistical Treatment of Orientational Ordering Using Mean-Field Approach	12
1.6.2 Anisotropic Intermolecular Interactions	14
1.6.3 Molecular Models of Orientational Order	15
A. Short-Range Models	15
B. Long-Range Models	17
1.6.4 Previous Predictions on Orientational Ordering	18
1.7 Outline of the Thesis	19
References	20

2	Experiment	22
	2.1 Sample Preparation	22
	2.2 Experimental Conditions	24
	References	26
3	Spectral Analysis	27
	3.1 Introduction	27
	3.2 Spectral Analysis with Aid of MQ NMR	27
	3.3 Molecular Structure and Order Parameters	40
	3.4 Summary	44
	References	44
4	Orientalional Ordering in Nematic Liquid Crystals	45
	4.1 Introduction	45
	4.2 Determination of a Consistent Set of Order Parameters	47
	4.3 Qualitative Comparison between Experimental Order Parameters	50
	4.4 Comparison between Experimental and Theoretically Calculated Order Parameters	52
	A. Short-Range Model Comparison	57
	B. Long-Range Model Comparison	58
	C. Dipolar Interaction Contribution	62
	D. Quadrupolar Interaction Contribution	62
	E. Polarizability Interaction Contribution	65
	4.4 Summary	67
	References	68
5	Conclusion	69

List of Tables

1.1	Independent Order Parameters as a Function of Molecular Symmetry	5
1.2	Maximum Number of Transitions in One Quantum Spectrum of a Partially Oriented Molecules as a Function of Number of Spins with $I = \frac{1}{2}$	10
3.1	Fitting Parameters and RMS Errors from Analysis of High-Resolution Spectra of TCB 3-spin System	30
3.2	Fitting Parameters from Analysis of MQ and High-Resolution Spectra of DCT in EBBA	32
3.3	Fitting Parameters and RMS Errors from Analysis of High-Resolution Spectra of DCT 6-spin System	37
3.4	Fitting Parameters and RMS Errors from Analysis of High-Resolution Spectra of CLMX 9-spin System	38
3.5	Fitting Parameters and RMS Errors from Analysis of High-Resolution Spectra of MESIT 12-spin System	39
3.6	Structural Parameters from Fits to Dipolar Couplings for DCT, CLMX and MESIT	41
3.7	Order Parameters from Fits to Dipolar Couplings	43
4.1	Scaled and Non-Scaled Order parameters	48
4.2	Anisotropy in Scale and Non-Scaled Order Parameters	51
4.3	Molecular Electrostatic Parameters	53
4.4	Adjusted Parameters in the Fitting Procedure	54

List of Figures

1.1	Liquid crystal phase on temperature scale	1
1.2	Example of nematic liquid crystal EBBA	2
1.3	Molecular organization in nematic phase	3
1.4	The nematic molecule fixed axis system	5
1.5	Poor resolved high-resolution spectrum of nematogen ZLI 1132	9
1.6	Three pulse sequence use to generate and observe MQ coherences	12
1.7	Elastic model for short-range interaction between solute and liquid crystal	16
2.1	ZLI 1132 liquid crystal	23
2.2	EBBA liquid crystal	23
2.3	Solutes	23
2.4	Single pulse sequence	24
2.5	3D MQ NMR pulse sequence	25
3.1	High-resolution proton NMR spectra of DCT, CLMX and MESIT in ZLI 1132 at 300K	29
3.2	All positive MQ spectra of DCT in EBBA at 300K	33
3.3	Experimental and calculated +5Q spectra of DCT in EBBA	34
3.4	Experimental and calculated +4Q spectra of DCT in EBBA	35
3.5	Experimental and calculated high-resolution proton spectra of DCT in EBBA at 300K	36
3.6	Atom labeling of solute molecules	42
4.1	Chosen set of solutes with same size and shape but different electrostatic properties presented in their coordinate system	46
4.2	Non-scaled (series A) and scaled (series B) experimental order parameters	49
4.3	Anisotropy in scaled order parameters	51
4.4	Differences between S_{xx}^{scaled} and S_{xx}^{calc} as a function of S_{xx}^{scaled} for short-range models	57
4.5	Differences between S_{xx}^{scaled} and S_{xx}^{calc} as a function of S_{xx}^{scaled} for long-range models	60
4.6	Different pair of short- with long-range interaction fits for magic mixture	61

4.7	Differences between S_{xx}^{scaled} and S_{xx}^{calc} as a function of S_{xx}^{scaled} for dipole interaction contribution	63
4.8	Differences between S_{xx}^{scaled} and S_{xx}^{calc} as a function of S_{xx}^{scaled} for quadrupole interaction contribution	64
4.9	Differences between S_{xx}^{scaled} and S_{xx}^{calc} as a function of S_{xx}^{scaled} for polarizability interaction contribution	66

List of Abbreviations

NMR	Nuclear magnetic resonance
MQ	Multiple quantum
Nematogen	Nematic liquid crystal molecule
ZLI 1132	Eutectic mixture of <i>trans</i> -4-n-alkyl-(4-cyanophenyl)-cyclohexane (alkyl=propyl, pentyl, heptyl) and <i>trans</i> -4-n-pentyl-(4'-cyanobiphenyl-4)-cyclohexane
EBBA	N-(p-EthoxyBenzylidene)-p'-n-ButylAniline
TCB	1,3,5 trichlorobenzene
DCT	3,5 dichlorotoluene
CLMX	5 chloro m-xylene
MESIT	1,3,5 trimethylbenzene (mesytilene)
<i>Efg</i>	Electric field gradient
\vec{n}	The director of liquid crystal
$S_{\alpha\beta}$	Order parameter
<i>x,y,z</i>	Molecule fixed axis system
<i>X,Y,Z</i>	Laboratory fixed axis system

Acknowledgements

I would like to thank my supervisor Prof. Elliott Burnell for his patience, encouragement, superb guidance and support over the past few years. It has been a great pleasure and privilege to work with him. I also wish to thank my colleagues Anand Yethiraj, Joseph Lee, Andrew Lewis, Ray Syvitski, Aman Taggar and Chris Campbell from which I have learned a lot and enjoyed interacting with. Thanks to Dr. Nick Burlinson for enthusiasm, moral support and resourceful discussions. Most of the experimental work wouldn't be possible without the excellent help from the people in the electronic shop, mechanical shop, chemistry store and NMR facility. I would also like to thank Scott Kroeker from University of Manitoba for donating one of the solutes, 3,5-dichlorobenzene. Financial assistance in the form of a teaching and research assistantship is highly appreciated.

Special thanks to my family for their love and support, since without their inspiration none of this would have been possible. Finally I would like to express my gratitude to my friends and loved one Ken for their constant support, help and patience.

Dedication

To my lovely parents

Ljiljana and Petar

1. INTRODUCTION

1.1 LIQUID CRYSTALS

The liquid crystal phase is known as a mesophase ($\mu\epsilon\sigma\sigma$ in Greek means middle), a phase between liquid and solid phases (Fig. 1.1). When heated from the solid phase at the first transition point they appear as a cloudy liquid that upon further heating above the clearing transition point transform into a clear isotropic liquid. Two transitional temperatures define the region in which mesophases are thermodynamically stable. Liquid crystals show the translational and rotational mobility of liquids and the optical properties of solids (like birefringence). They typically consist either of rod like or disk like molecules.

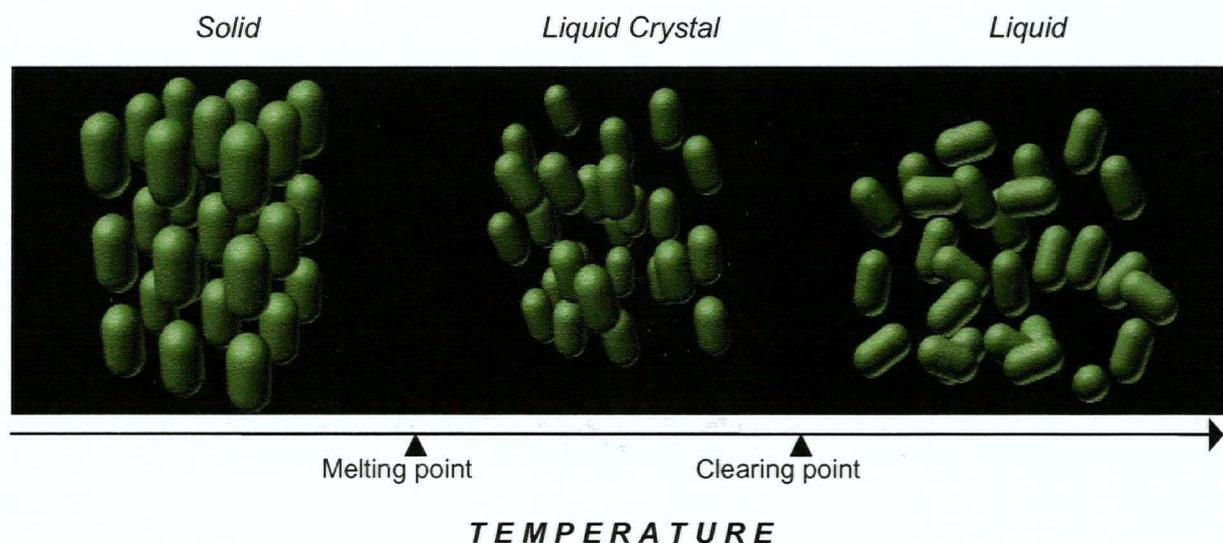


Figure 1.1 Liquid crystal phase on temperature scale

The main characteristic of liquid crystals is long-range orientational ordering. Some of them display some positional ordering as well.

The tendency to align along a preferred direction is caused by intermolecular forces acting between liquid crystal molecules. As a consequence liquid crystals are categorized as anisotropic phases in which measured properties depend on the direction in which they are measured. The anisotropic nature of liquid crystals is responsible for their unique properties exploited in a variety of applications.

Liquid crystals are classified into two main categories: thermotropic and lyotropic.

Thermotropic liquid crystals are produced by thermal process as while lyotropic liquid crystal phases depend on solvent composition.

The present study focuses only on nematic liquid crystals, the simplest thermotropic liquid crystal that possesses only orientational order.

1.2 NEMATIC LIQUID CRYSTALS

Nematic (*νεματωσ* in Greek means threadlike) liquid crystals are composed of rod-shaped molecules with molecular length several times the molecular diameter. These molecules consist of semi-rigid cores like benzene rings with polar and nonpolar flexible ending groups (Fig. 1.2).

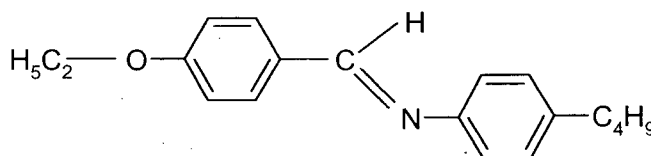


Figure 1.2 Example of nematic liquid crystal EBBA (N-(p-Ethoxybenzylidene)-p'-nButyl Aniline); stable in the temperature range from 308 to 352 K

Nematic molecules (*nematogens*) are arranged such that there is no positional order of their centers of mass, meaning that molecules diffuse randomly and rapidly like in isotropic liquids. When a solid melts the thermal energy is sufficient to destroy positional order but not enough to disrupt orientational order. This results in a nematic phase in which molecules group in clusters, and tend to partially align their molecular axes along a preferred direction, called the director \vec{n} (Fig. 1.3). The cluster size can be as large as $1 \mu m$ [1].

In the absence of an external field, the orientation of the director axis in each cluster varies throughout the sample. The cloudy appearance of a macroscopic sample comes from the random scattering of light as it penetrates the sample between the clusters with different directors. In the presence of a magnetic field all clusters' directors reorient along the main magnetic field direction in just a few seconds. For almost all nematics known nowadays, the nematic phase is uniaxial.

Therefore they are cylindrically symmetric and all measured properties are invariant to rotations about the director \vec{n} . Also the directions $-\vec{n}$ and \vec{n} are indistinguishable making the phases apolar.

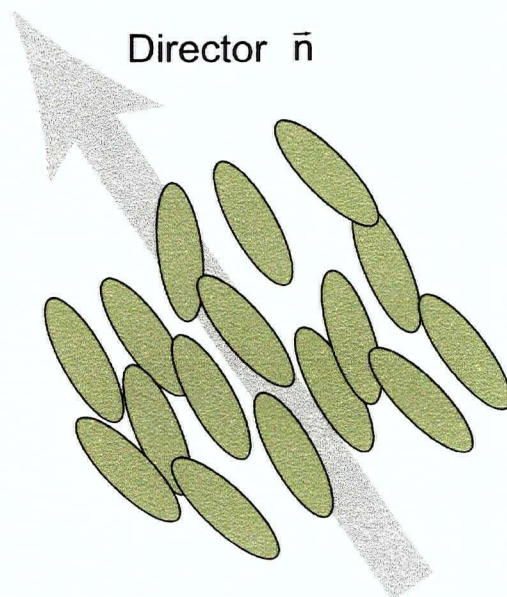


Figure 1.3 Molecular organization in nematic phase

1.3 ORIENTATIONAL ORDERING AND INTERMOLECULAR FORCES IN NEMATIC LIQUID CRYSTALS

Orientalional order is one of the basic characteristics common to all the mesophases. It is a result of anisotropic intermolecular forces acting between liquid crystal molecules.

Understanding the relationship between orientational order and anisotropic intermolecular forces that cause the molecular orientation is one of the fundamental questions in the study of liquid crystals that still hasn't been fully answered.

Several approaches (experimental, theoretical and computational) have been utilized in order to give some insight into the problem. In this study, NMR was used to extract information about order parameters that were compared with theoretically predicted order parameters calculated from theoretical models (which will be described in 1.6).

1.4 ORIENTATIONAL DISTRIBUTION FUNCTION AND ORDER PARAMETER

/quantitative description of orientational order/

The orientational behaviour of a *rigid, axially symmetric nematogen* is fully described by the single orientational distribution function $f(\Omega)$, where Ω represents the Eulerian angles (φ, θ, ψ) that describe the orientation of the molecule frame system (x, y, z) relative to the nematic director system (laboratory frame system (X, Y, Z)) (Fig. 1.4). Taking into account the cylindrical symmetry and uniaxiality of the phase, the orientational distribution function $f(\Omega)$, expanded in terms of spherical harmonics, reduces to [2]:

$$f(\Omega) = \sum_{l \text{ even}} \frac{2l+1}{2} \langle P_l \rangle P_l(\cos\theta) = \frac{1}{2} + \frac{5}{2} \langle P_2 \rangle P_2(\cos\theta) + \frac{9}{2} \langle P_4 \rangle P_4(\cos\theta) + \dots \quad (1.1)$$

where

$$\langle P_l \rangle = \int_0^\pi P_l(\cos\theta) f(\theta) \sin\theta d\theta \quad (1.2)$$

are called *orientational order parameters* and P_l are Legendre polynomials [2].

The same concept can be applied to describe the orientational behavior of an axially symmetric rigid solute molecule dissolved in a liquid crystal.

Second rank order parameters also known as components of the Saupe order matrix represent quantitative measures of average orientational order of rigid molecules of any symmetry in anisotropic systems [3]. The order matrix is a 3x3 symmetric ($S_{\alpha\beta} = S_{\beta\alpha}$) and traceless ($\sum_{\alpha=\beta} S_{\alpha\beta} = 0$) matrix with five independent components. The matrix elements $S_{\alpha\beta}$

in the Cartesian coordinate representation are given as

$$S_{\alpha\beta} = \langle P_2 \rangle = \frac{\langle 3 \cos\theta_\alpha \cos\theta_\beta - \delta_{\alpha\beta} \rangle}{2} \quad (1.3)$$

where α and β are the molecular fixed axes conveniently chosen as symmetry axes of the molecule; θ_α and θ_β are angles between α and β molecular axis and the nematic director (which usually coincides with the magnetic field direction) (Fig. 1.4).

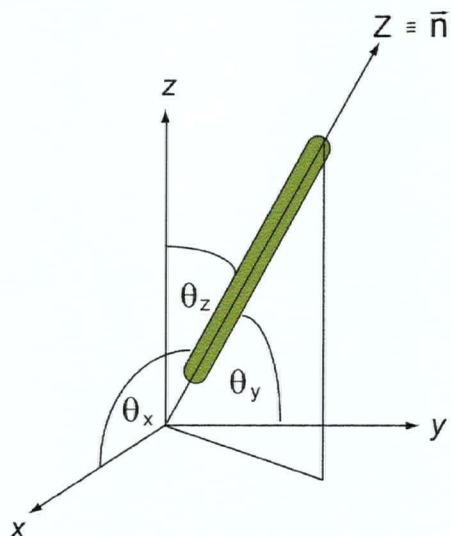


Figure 1.4 The nematic molecule fixed axis system

The nematic director \vec{n} and magnetic field \vec{B}_0 direction are parallel to the laboratory fixed Z direction

Suitably choosing molecular axes, the number of independent order parameters can be reduced depending on the symmetry of the molecule (Table 1.1) [4,5].

Table 1.1 Independent Order Parameters as a Function of Molecular Symmetry

Symmetry point group	Independent order parameters
$C_n, C_{nv}, C_{nh}, C_{\infty h} (n = 3 - 6)$	S_{zz}
$D_n, D_{nh}, D_{\infty h} (n = 3 - 6)$	
$D_{nd} (n = 2 - 5), S_4, S_6$	
C_{2v}, D_2, D_{2h}	$S_{zz}, S_{xx} - S_{yy}$
C_s, C_2, C_{2h}	S_{xx}, S_{yy}, S_{xy}
C_1, C_i	$S_{xx}, S_{yy}, S_{xy}, S_{xz}, S_{yz}$

Equation (1.3) defines the range of order parameter values:

for diagonal order parameter elements

$$-\frac{1}{2} \leq S_{\alpha\alpha} \leq 1 \quad (1.4)$$

and for off-diagonal order parameter elements

$$-\frac{3}{4} \leq S_{\alpha\beta} \leq \frac{3}{4} \quad (1.5)$$

When all molecules are oriented parallel to the magnetic field and therefore the nematic director ($\theta = 0$ or $\theta = \pi$), the order parameter is $S_{\alpha\alpha} = 1$ indicating perfect alignment while for perpendicular alignment ($\theta = \frac{\pi}{2}$), the order parameter becomes $S_{\alpha\alpha} = -\frac{1}{2}$. If molecules tumble freely and isotropically orientation is totally random, the average value of the cosine squared function is $\langle \cos^2 \theta \rangle = \frac{1}{3}$ and $S_{\alpha\alpha} = 0$, i.e. the system shows no orientational order at all.

1.5 ORIENTATIONAL ORDERING FROM EXPERIMENTS

There are many experimental techniques that can provide information about orientational ordering. For example polarized Raman scattering [6], Electron Paramagnetic Resonance (EPR) [7], quasielastic scattering of X-rays [8] or neutrons [9] can give up to fourth rank orientational order parameters. Their instrumental and analytical limitations make this task really difficult and incomplete. NMR has proved to be an excellent non-destructive technique for studying orientational order in anisotropic systems. Its only limitation lies in the fact that only the second rank order parameters can be extracted from experimental NMR spectroscopic data therefore giving a slightly modest representation of the orientational distribution function. The theoretical background and the relationship between order parameters and accessible spectral parameters will be described in the following section 1.6.1. Spectral step by step analysis and determination of order parameters will be covered in Chapter 3.

1.5.1 NMR SPECTRA OF ORIENTED MOLECULES

In the high-field limit* the spin Hamiltonian for a collection of spins ($I = \frac{1}{2}$) in a uniaxial anisotropic environment is given as:

$$\hat{H} = \hat{H}_Z + \hat{H}_J + \hat{H}_D \quad (1.6)$$

where \hat{H}_Z is the Zeeman, \hat{H}_J is the scalar (indirect) coupling and \hat{H}_D is the direct dipolar Hamiltonian.

The Zeeman Hamiltonian represents the interaction between nuclei and the main external magnetic field. Expressed in Hz units, it takes the following form

$$\hat{H}_Z = -\sum_i \nu_i I_{i,z} = -\frac{B_Z}{2\pi} \sum_i \gamma_i (1 - \sigma_{i,ZZ}) I_{i,z} \quad (1.7)$$

where ν_i are the chemically shifted frequencies of the i spin, B_Z is the static external magnetic field defined to be along the Z-axis, $I_{i,z}$ is the Z-component of the spin operator for the i spin, and $\sigma_{i,ZZ}$ is the ZZ-component of the chemical shift tensor for spin i .

The scalar coupling Hamiltonian has the general form

$$\hat{H}_J = \sum_{i < j} \vec{I}_i \cdot J_{ij} \cdot \vec{I}_j \quad (1.8)$$

where the scalar coupling constant J_{ij} is a second-rank tensor that describes the indirect interaction between spins defined through spin operators \vec{I}_i and \vec{I}_j .

Another approximation is applied here: for most protons the anisotropy in the J_{ij} tensor is small and is ignored.

* The high-field limit approximation takes into account that the Zeeman term in the Hamiltonian dominates over other terms in the Hamiltonian; for example the Zeeman term in a 100 MHz field is of order $\sim 10^8$ Hz while dipolar and quadrupolar contributions do not exceed 10^4 Hz; this simplifies the expression for the Hamiltonian.

The direct dipolar Hamiltonian

$$\hat{H}_D = \sum_{i < j} D_{ij} (3I_{i,Z}I_{j,Z} - \vec{I}_i \cdot \vec{I}_j) \quad (1.9)$$

takes into account the interaction between magnetic dipoles of spins i and j through the dipolar coupling constant D_{ij} given as

$$D_{ij} = -\frac{\mu_0 \hbar \gamma_i \gamma_j}{8\pi^2} \left\langle \frac{\frac{3}{2} \cos^2 \theta_{ij,Z} - \frac{1}{2}}{r_{ij}^3} \right\rangle \quad (1.10)$$

where μ_0 is the magnetic permeability of vacuum, \hbar is Planck's constant, γ is the gyromagnetic ratio of the spin and $\theta_{ij,Z}$ is the angle between the internuclear vector r_{ij} and the external magnetic field defined along the Z-axis. For rigid molecules (i.e. ignoring vibrations and taking r_{ij} fixed instead of using the averaged values for $\left\langle \frac{1}{r_{ij}^3} \right\rangle$) expression

(1.10) can be rewritten as

$$D_{ij} = -\frac{\mu_0 \hbar \gamma_i \gamma_j}{8\pi^2 r_{ij}^3} \sum_{\alpha\beta} S_{\alpha\beta} \cos \vartheta_\alpha \cos \vartheta_\beta \quad (1.11)$$

where $S_{\alpha\beta}$ are the order matrix elements and $\vartheta_\alpha, \vartheta_\beta$ are angles between α, β molecular axes and the internuclear vector r_{ij} . Equation (1.11) is the basis for the experimental NMR study of orientational order. It gives a direct relation between extractable spectral information (D_{ij}) and second-rank orientational order parameters as a measure of orientational order of the molecule in anisotropic media.

In isotropic media, rapid translational motion and random reorientation cause intermolecular and intramolecular dipolar interactions to average out ($D_{ij}=0$), due to which isotropic spectra look less complicated and give no information about orientational order.

The eigenstates and eigenvalues are obtained from a diagonalization of the Hamiltonian. They are characterized by spectral parameters $(\sigma, J_{ij}D_{ij})$ in the Hamiltonian. On the other side eigenvalues and eigenstates govern spectral frequencies and intensities and make the connection between accessible spectral parameters and actual spectra.

1.5.2 SOLUTES AS PROBES OF ORIENTATIONAL ORDER AND INTERMOLECULAR FORCES

Increasing the number of spins in a molecule causes the number of dipolar couplings to rise which results in very complex, poorly resolved high-resolution spectra that are hard to analyze and extract spectral information from. That kind of situation is present in high-resolution spectra of nematogens, since individual molecules might have more than 20 proton spins (Fig.1.5).

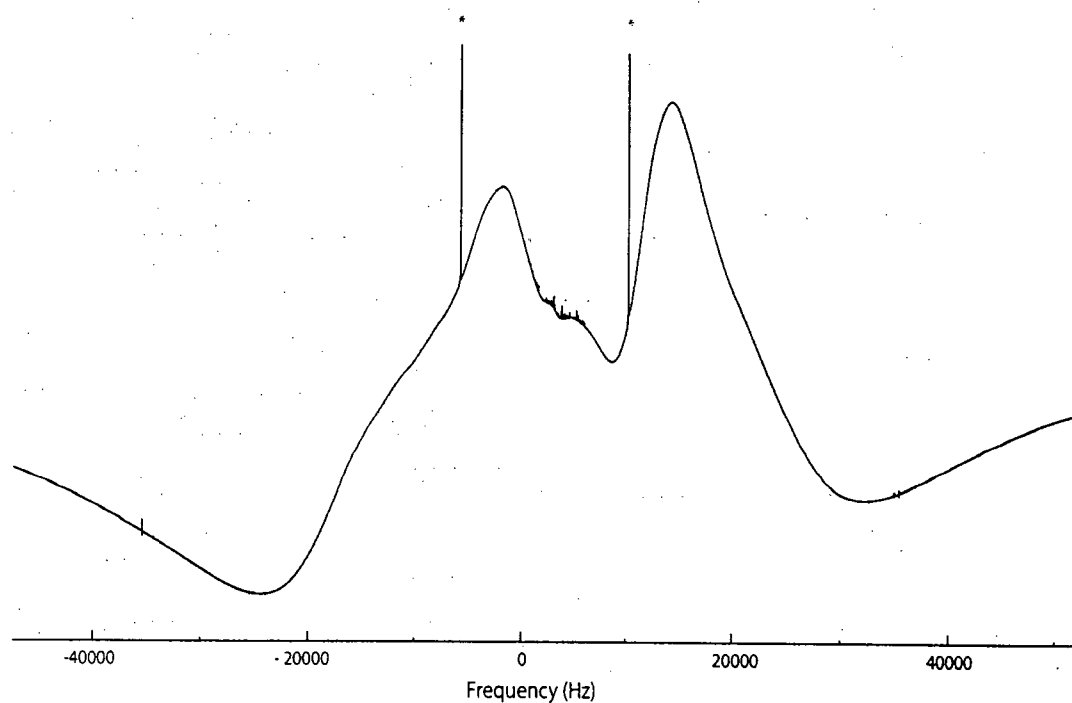


Figure 1.5 Poor resolved high-resolution NMR spectrum of nematogen ZLI 1132

Spectral lines marked as (*) belong to impurities used to stabilize the system

A very useful alternative for studying orientational order in nematic liquid crystals is to use solutes as probes of orientational order.

Usually small, rigid symmetric molecules are used to simplify spectral analysis. They are dissolved in the liquid crystal in small concentrations to avoid any strong perturbations in the liquid crystal environment. Addition of small amounts of solutes only changes physical properties of the liquid crystal (such as the nematic-isotropic transition temperature) but the fundamental nature of liquid crystals stays unchanged. Also solutes feel the same orientational forces as liquid crystal molecules themselves.

Another important reason why this approach of using small, symmetric molecules is very useful is that by choosing certain types of molecules it is possible to explore the role of particular intermolecular forces in orientational ordering mechanisms. This can be achieved by choosing a solute with a particular property [10], or by choosing a set of solutes whose properties vary in a well-characterized way [11,12], or by choosing a liquid crystal solvent that has special properties [10].

1.5.3 MULTIPLE QUANTUM NMR

/spectral simplification and analysis of high-resolution NMR spectra/

High-resolution proton NMR spectra ($\Delta M = \pm 1$) of low spin systems are relatively solvable without too much trouble. They might have hundreds of lines. The number of single transitions for an N spin system that has 2^N distinct eigenstates and eigenvalues can be calculated as

$$\text{Number of transitions} = \frac{(2N)!}{(N-1)!(N+1)!} \quad (1.12)$$

Table 1.2 Maximum Number of Transitions in One Quantum Spectrum of a Partially Oriented Molecule as a Function of Number of Spins with $I = \frac{1}{2}$

Number of spins	1	2	3	4	5	6	7	8
Number of transitions	1	4	15	56	210	792	3003	11000

For systems that have some degree of symmetry (Table 1.1) many energy levels with the same M quantum number are degenerate which automatically reduces the possible number of transitions and therefore simplifies the spectra.

Many spin systems with $N > 8$ have a complex Hamiltonian and high-resolution NMR spectra which are challenging to analyze even for symmetric molecules. For these systems which have so closely packed spectra, quite accurate initial spectral parameters are required in order to solve the spectrum. In that case known spectral parameters (D_{ij} , J_{ij} and σ_i) of molecules with similar size and shape for the same liquid crystal are used as starting parameters in spectral analysis. In most cases this does not lead to a satisfactory solution so multiple quantum NMR is used.

Multiple quantum spectra involve transitions between energy levels with the difference in M quantum numbers $\Delta M = 0, \pm 1, \dots, \pm(N-1), \pm N$. Higher order multiple quantum spectra are quite simple containing fewer transitions than lower quantum ($\Delta M < \pm(N-2)$) spectra and therefore easier to analyze.

Transition frequencies are governed by the same spectral parameters as conventional high-resolution spectra. In principle analyzing the N, N-1 and N-2 multiple quantum spectra is sufficient enough to gather all spectral parameters. The limitation of MQ NMR lies in the fact that multiple quantum spectra are much broader and less resolved than single quantum spectra leading to less precise spectral parameters. That is why spectral parameters determined from MQ experiments are used as initial spectral parameters in analysis of high-resolution spectra.

Generally MQ coherences are created and observed using a three pulse sequence (Fig. 1.5) [13]. Before firing the first pulse the spin system is in equilibrium and only longitudinal magnetization $\overline{I_z}$ is present. The first pulse flips $\overline{I_z}$ magnetization into the x-y plane, which evolves in preparation time τ (fixed) among one-quantum coherences.

The second pulse transforms one-quantum coherences into all possible MQ coherences that evolve in $t1$ evolution time under the internal spin Hamiltonian (direct dipolar, indirect scalar) and finally the third pulse partially converts MQ coherences back into observable $\overline{I_z}$ one-quantum coherences that evolve in time $t2$.

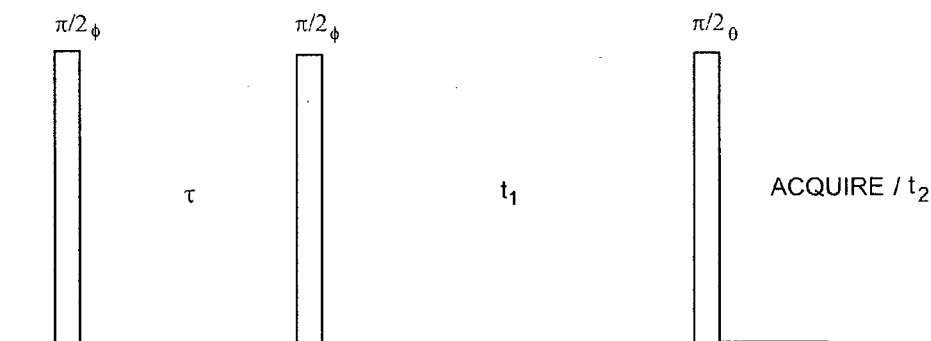


Figure 1.6 Three pulse sequence used to generate and observe MQ coherences

More on how different MQ coherences are selectively detected using phase cycling and how MQ spectra are transformed will be explained in Chapter 2.

1.6 ORIENTATIONAL ORDERING FROM THEORETICAL CALCULATION

1.6.1 STATISTICAL TREATMENT OF ORIENTATIONAL ORDERING USING MEAN-FIELD APPROACH

The orientational distribution function $f(\Omega)$ fully describes the orientational order of a rigid solute in the nematic liquid crystal as well as the connection with experimentally measurable spectral parameters. Using statistical mechanics, the orientational distribution function $f(\Omega)$ can be expressed as a singlet distribution function, that is

$$f(\Omega) = \frac{e^{\frac{U(\Omega)}{kT}}}{\int e^{\frac{U(\Omega)}{kT}} d\Omega} \quad (1.13)$$

In the mean-field approximation all interactions in the system can be represented as interactions between a single molecule and the average field, i.e. $U(\Omega)$ is the mean-field potential that governs the orientational order of the molecule.

The physical picture behind this simple philosophy is that interactions between the solute and the liquid crystal environment (solvent) are described as interactions between a solute property (such as dipole) and the averaged field of the solvent, so that

$$U(\Omega) = A_{Solute}(\Omega) \cdot F_{Liquid\ crystal} \quad (1.14)$$

The assumption that the averaged field is not influenced by the solute presence means that there is a clear and distinct separation of both solute and solvent contributions to the potential (no correlations between the two contributions).

Statistically speaking, any measurable property taken as an average (for example $S_{\alpha\beta}$) can be then expressed as

$$S_{\alpha\beta} = \int f(\Omega) \cdot \left(\frac{3}{2} \cos\theta_\alpha \cos\theta_\beta - \frac{1}{2} \delta_{\alpha\beta}\right) \cdot d\Omega \quad (1.15)$$

Combining Eq. 1.3, 1.13 and 1.15 gives

$$S_{\alpha\beta}^{calc} = \frac{\int \left(\frac{3}{2} \cos\theta_\alpha \cos\theta_\beta - \frac{1}{2} \delta_{\alpha\beta}\right) \cdot e^{-\frac{U(\Omega)}{kT}} d\Omega}{\int e^{-\frac{U(\Omega)}{kT}} d\Omega} \quad (1.16)$$

Equation 1.16 is the basis for the statistical treatment of the orientational ordering, because it connects the intermolecular potential with the orientational ordering. It gives the opportunity to investigate various intermolecular potentials, by comparing calculated and experimental order parameters and therefore create a better picture of the orientational behavior of molecules in nematic liquid crystals. Representation of the intermolecular interactions can be done either using statistical theories (Maier-Saupe [14,15], Onsager [16]), simulation methods [17-25] or phenomenological models [10-12,26-29]. In the present study the simple phenomenological approach will be utilized.

1.6.2 ANISOTROPIC INTERMOLECULAR INTERACTIONS

Anisotropic intermolecular interactions are responsible for the orientational ordering of the solutes in the liquid crystal systems. The effective orienting mean-field potential can be divided into two contributing terms; one that presents short-range interactions and the other that presents long-range interactions, so that

$$U(\Omega) = U(\Omega)^{SR} + U(\Omega)^{LR} \quad (1.17)$$

Short-range interactions consist of both an attractive and repulsive part. At short distances, the attractive part is ignored. Only the dominant repulsive part that is a consequence of overlapping of the electron clouds between neighbour molecules is considered. Short-range interactions are considered as interactions that are highly affected by the molecular structure.

Long-range interactions involve distances much larger than the molecular dimensions. They are attractive or repulsive interactions that depend on electrostatic properties of the molecules.

1.6.3 MOLECULAR MODELS OF ORIENTATIONAL ORDER

A. SHORT-RANGE MODELS

A1. CI model

One of the short-range potentials used is a phenomenological model called CI by Burnell and co-workers [10], a combination of a circumference (C) model and an integral (I) model [26, 27] in which

$$U(\Omega)_{CI}^{SR} = \frac{1}{2}k_{ZZ} \left(k(C(\Omega))^2 - k_s \int_{Z_{\min}}^{Z_{\max}} C(Z, \Omega) dZ \right) \quad (1.18)$$

where k_{zz} is a solvent parameter that determines the mean field influence on the solute, k and k_s are proportionality constants; $C(\Omega)$ is the circumference of the projection of the solute at orientation Ω onto a plane perpendicular to the director (that is along the Z axis in the laboratory frame) and $C(\Omega, Z)$ is the circumference of the projection of the solute at position Z and orientation Ω onto a plane perpendicular to the director; so that $C(\Omega, Z) dZ$ is an infinitesimal thin ribbon that traces out the molecule at position Z and orientation Ω .

The first term in Eq. 1.18 (C model) can be interpreted as a Hooke's elastic law where the liquid crystal is treated as an elastic continuum and the solute as its distortion. The second term (I model) can be seen as an anisotropic interaction between solute surfaces and solvent averaged field. The presented model treats molecules as a collection of van der Waals hard spheres placed at the atomic sites (Fig. 1.7).

A2. SS model

Another type of short-range potential written as an expansion in spherical harmonics truncated at the first non-zero term [11] is

$$U(\Omega)_{SS}^{SR} = -\frac{1}{2} \sum_{\alpha, \beta=x, y, z} (M_{\alpha\beta} k_{zz}) (3 \cos\theta_{\alpha} \cos\theta_{\beta} - \delta_{\alpha\beta}) \quad (1.19)$$

where $M_{\alpha\beta}$ are the traceless tensor components related to size and shape, and k_{zz} is the same as in the previous model, a liquid crystal parameter related to the degree of orientation of the nematogen.

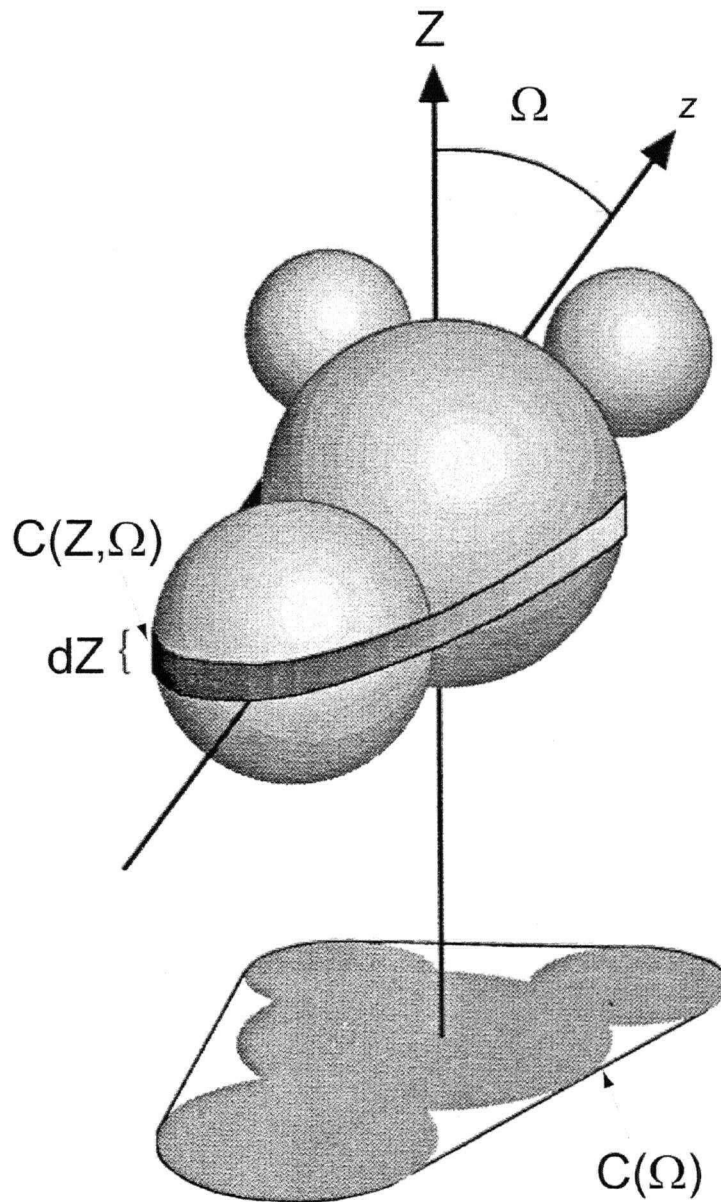


Figure 1.7 Elastic model for short-range interaction between solute and liquid crystal. The potential described by Eq. 1.18 depends on the orientation Ω of the molecule throughout $C(\Omega)$ and $C(Z, \Omega)$; $C(\Omega)$ is the circumference of the projection of the solute at orientation Ω onto a plane perpendicular to the director; $C(Z, \Omega)$ is the circumference of the projection of the solute at position Z and orientation Ω onto a plane perpendicular to the director. The Z axis corresponds to the direction of the liquid crystal director. The molecules are modeled as a collection of van der Waals hard spheres.

B. LONG-RANGE MODELS

For long-range models only dipoles, quadrupoles and polarizabilities are suspected to be the most important contributors to orientational ordering and therefore will be utilized.

B1. Dipole model

The dipole interaction in the mean-field approximation, defined as an interaction between a permanent solute dipole moment and the averaged electric field of the liquid crystal, would be zero due to the apolar nature of the liquid crystal, *i.e.* $\langle E \rangle \equiv 0$. Nevertheless, the permanent dipole moment can induce a dipole moment in the liquid crystal, creating the so called *reaction field* (in the liquid crystal) that will in return react with the permanent dipole. The magnitude of this kind of interaction is proportional to the magnitude of the created field as can be seen from:

$$U(\Omega)_{Dipole}^{LR} = -\frac{1}{4\pi\epsilon_0} \frac{1}{6} \sum_{\alpha,\beta=x,y,z} \mu_\alpha \mu_\beta \langle \bar{R}_{ZZ} - \bar{R}_{XX} \rangle (3 \cos\theta_\alpha \cos\theta_\beta - \delta_{\alpha\beta}) \quad (1.20)$$

where μ_α, μ_β are dipole moments of the solute along the α, β molecule fixed directions and $\langle \bar{R}_{ZZ} - \bar{R}_{XX} \rangle$ is the average value of the difference in the electric field between the Z and X laboratory directions [11,12].

B2. Quadrupole model

The quadrupole interaction, an interaction between the quadrupole moment of the solute and the electric field gradient of the liquid crystal (*efg*), is given by

$$U(\Omega)_{Quadrupole}^{LR} = -\frac{1}{4\pi\epsilon_0} \frac{1}{6} \sum_{\alpha,\beta=x,y,z} (Q_{\alpha\beta} \bar{F}_{ZZ}) (3 \cos\theta_\alpha \cos\theta_\beta - \delta_{\alpha\beta}) \quad (1.21)$$

where $Q_{\alpha\beta}$ is the $\alpha\beta$ quadrupole tensor component of the solute and \bar{F}_{ZZ} is the ZZ component of the electric field gradient, traceless second-rank tensor parallel to the nematic director [11].

B3. Polarizability model

The local electric fields within the liquid crystals could change the electronic charge distribution in the solute molecules that could lead to a change in their orientation. The potential corresponding to this kind of interaction is:

$$U(\Omega)_{Polarizability}^{LR} = -\frac{1}{4\pi\epsilon_0} \frac{1}{6} \sum_{\alpha, \beta=x, y, z} \alpha_{\alpha\beta} \langle \bar{E}_{ZZ}^2 - \bar{E}_{XX}^2 \rangle (3 \cos\theta_\alpha \cos\theta_\beta - \delta_{\alpha\beta}) \quad (1.22)$$

where $\alpha_{\alpha\beta}$ is the $\alpha\beta$ molecular polarizability tensor component of the solute and $\langle \bar{E}_{ZZ}^2 - \bar{E}_{XX}^2 \rangle$ is the average value of the squares of the electric field between the Z and X laboratory directions [11].

1.6.4 PREVIOUS PREDICTIONS ON ORIENTATIONAL ORDERING

Some important experiments and predictions from theory/models over the course of the past few decades will be presented so as to gain a better perspective on where the science stands on the fundamental question of orientational ordering.

Phenomenological investigation of orientational ordering has been developed in two different ways. One in which interactions between solutes and liquid crystals are described as mean-field interactions meaning that all solutes feel the same averaged liquid crystal field [12, 30-36]. The other states that the mean-field picture is too simple and that there are correlation effects between solutes and liquid crystals leading to the fact that different solutes feel different liquid crystal fields [37-39]. This is supported by the possibility that one solute molecule could spend more time on average in the aromatic regions of the liquid crystals while the other solute would prefer more the hydrocarbon chain region of the liquid crystals.

Burnell and co-workers have utilized the mean-field approach and investigated the orientational behaviour of small symmetric molecules D_2 and HD [30-33] and methane [34-36] in a special mixture called *magic mixture* of 55 wt% 1132/EBBA and its pure components. From magic mixture experiments it was determined that there is no long-range

interaction contributions to the ordering, leaving the short-range interaction as the dominant contribution. The same results were obtained studying a whole range of small molecules dissolved in the magic mixture [12]. A computer simulation study of hard ellipsoids was performed to test the previously stated findings, and confirmed that short-range interactions indeed have a dominant effect on the orientational ordering of molecules in liquid crystals [19]. Studies of D_2 and HD in pure component liquid crystals show some evidence of quadrupole-liquid crystals efg interactions. The determined electric field gradient of EBBA was shown to be negative not only from D_2 and HD but also from benzene and benzene derivatives studies [12]. The sign of the efg of EBBA is the same as one predicted from the mean-field quadrupole moment/ efg model demonstrating that the quadrupole interaction is an important orientational mechanism.

Photinos *et al.* [37-39] on the contrary predicted theoretically that short- and long-range interactions contribute equally to the orientation and that long-range interactions arise mainly from dipoles and quadrupoles.

Emsley, Luckhurst and co-workers have shown, using the statistical Maier-Saupe theory of nematics [40-42] that the quadrupole is the lowest order multipole that contributes to a non-vanishing efg and that the efg strongly depends on solute and solvent molecular properties. Overall agreement of different results from experiments, theories and computer simulations is that short-range interactions, size and shape dependent, are the dominant orientational mechanism. The importance of different electrostatic interactions is still an open question and is the main object of the presented study.

1.7 THE OUTLINE OF THE THESIS

In order to gain a better understanding about anisotropic intermolecular forces within liquid crystals, small molecules were dissolved in liquid crystal solvents and used to probe the anisotropic intermolecular forces. Chosen solute molecules have the same size and shape, same short-range contribution to the ordering but different electrostatic properties that enable testing of the effects of the additional long-range interactions. Also, the choice of liquid crystals is important in the sense of separately exploring the effects of different electrostatic effects. In magic mixture liquid crystals it was found [30-33] that the efg is zero, i.e. quadrupole interactions are annulled and therefore other electrostatic effects (like dipole and polarizability) if effective should clearly be visible.

Chapter 1 contains all the theory basics needed to understand the experimental and theoretical determination of the spectral and order parameters and how valuable information about intermolecular forces that causes the orientational behavior of the molecules in liquid crystals can be extracted from those parameters.

Chapter 2 presents the technical aspect of experiments while Chapter 3 focuses on analysis methodology and determination of spectral and structural parameters from non-vibrationally corrected dipolar couplings.

A set of self-consistent order parameters is obtained in Chapter 4 and it was used to examine the effects of various short- and long-range interactions models on the ordering by comparing them with the calculated order parameters from those models.

Chapter 5 summarizes the important results of the presented study with future work proposal.

References:

- [1] de Gennes, P. and Prost, J., 1993, *The Physics of Liquid Crystals*, Clarendon Press, Oxford, 2nd edition.
- [2] Emsley, J. W., 1985, *Nuclear Magnetic Resonance of Liquid Crystals*, C. Riedel Press
- [3] Saupe, A., 1964, *Z. Naturforsch.*, **19**, 161.
- [4] Diehl, P., Khetrpal, C. I., 1969, *NMR Basic Principles and Progress*, Vol. 1, Springer-Verlag, Berlin.
- [5] Burnell, E. E., de Lange, C. A., 2003, *NMR of Ordered Liquids*, Kluwer Academic Publishers.
- [6] Vartogen, G. and de Jeu, W. H., 1988, *Thermotropic Liquid Crystals, Fundamentals*, Springer-Verlag.
- [7] Berliner, L. J., 1976, *Spin Labelling: Theory and Application*, Academic Press, London.
- [8] Zannoni, C. and Guerra, M., 1981, *Mol. Phys.*, **44**, 849.
- [9] Leadbetter, A., 1979, *The Molecular Physics of Liquid Crystals*, Academic Press.
- [10] Burnell, E. E. and de Lange, C., 1998, *Chem. Rev.*, **98**, 2359.
- [11] Syvitski, R. and Burnell, E. E., 1997, *Chem. Phys. Letters*, **281**, 199.
- [12] Syvitski, R. and Burnell, E. E., 2000, *J. Chem. Phys.*, **113**, 3452.
- [13] Syvitski, R., Burlinson, N., Burnell, E. E. and Jeener, J., 2002, *J. Mag. Res.*, **155**, 251.
- [14] Maier, W. and Saupe, A., 1959, *Z. Naturforsch. A*, **14**, 287.

- [15] Maier, W. and Saupe, A., 1960, *Z. Naturforsch. A*, **15**, 882.
- [16] Onsager, L., 1949, *N.Y. Acad. Sci.*, **51**, 627.
- [17] Hashim, R., Luckhurst, G. R. and Romano, S., 1985, *Mol. Phys.*, **56**, 1217.
- [18] Luzar, M. Rosen, M. E. and Caldarelli, S., 1996, *J. Phys. Chem.*, **100**, 5098.
- [19] Polson, J. M. and Burnell, E. E., 1996, *Mol. Phys.*, **88**, 767.
- [20] Polson, J. M. and Burnell, E. E., 1997, *Phys. Rev. E*, **55**, 4321.
- [21] Syvitski, R. T., Polson, J. M. and Burnell, E. E., 1999, *Int. J. Mol. Phys. C*, **10**, 403.
- [22] Burnell, E. E., Berardi, R., Syvitski, R. T. and Zannoni, C., 2000, *Chem. Phys. Letters*, **331**, 455.
- [23] Celebre, G., 2001, *Chem. Phys. Letters*, **342**, 375.
- [24] Celebre, G., 2001, *J. Chem. Phys.*, **115**, 9552.
- [25] Lee, J. -S. J., Undergraduate thesis, Department of Chemistry, University of British Columbia, 2001.
- [26] van der Est, A. J., Kok, M. Y. and Burnell, E. E., 1987, *Mol. Phys.*, **60**, 397.
- [27] Zimmerman, D. S. and Burnell, E. E., 1990, *Mol. Phys.*, **69**, 1059.
- [28] Zimmerman, D. S. and Burnell, E. E., 1993, *Mol. Phys.*, **78**, 687.
- [29] Ferrarini, A., Moro, G. J., Nordio, P. L. and Luckhurst, G. R., 1992, *Mol. Phys.*, **77**, 1.
- [30] Burnell, E. E., de Lange, C. A. and Snijders, J. G., 1982, *Phys. Rev.*, **A25**, 2339.
- [31] Burnell, E. E., van der Est, A. J., Patey, G. N., de Lange, C. A. and Snijders, J. G., 1987, *Bull. Mag. Reson.*, **9**, 4.
- [32] van der Est, A. J., Burnell, E. E. and Lounila, J., 1988, *J. Chem. Soc. Faraday Trans. 2*, **84**, 1095.
- [33] Burnell, E. E., de Lange, C. A., Serge, A. L., Capitani, D., Angelini, G., Lilla, G. and Barnhoorn, J. B. S., 1997, *Phys. Rev.*, **E55**, 496.
- [34] Snijders, J. G., de Lange, C. A. and Burnell, E. E., 1983, *Israel. J. Chem.*, **23**, 269.
- [35] Snijders, J. G., de Lange, C. A. and Burnell, E. E., 1982, *J. Chem. Phys*, **77**, 5386.
- [36] Snijders, J. G., de Lange, C. A. and Burnell, E. E., 1983, *J. Chem. Phys*, **79**, 2964.
- [37] Terzis, A. and Photinos, D., 1994, *Mol. Phys.*, **83**, 847.
- [38] Photinos, D., Poon, C., Samulski, E. and Toiumi, H., 1992, *J. Phys. Chem*, **96**, 8176.
- [39] Photinos, D., Poon, C., Samulski, E., 1993, *J. Chem. Phys.*, **98**, 10009.
- [40] Emsley, J., Palke, W. and Shilstone, G., 1991, *Liquid Crystals*, **9**, 643.
- [41] Emsley, J., Heeks, S., Horne, T., Howells, M., Moon, A., Palke, W., Patel, S., Shilstone, G. and Smith, A., 1991, *Liquid Crystals*, **9**, 649.
- [42] Emsley, J., Luckhurst, G. and Sachdev, H., 1989, *Mol. Phys.*, **67**, 151.

2. EXPERIMENT

2.1 SAMPLE PREPARATION

The nematic liquid crystals used as solvents are:

~ ZLI-1132, a eutectic mixture of *trans*-4-n-alkyl-(4-cyanophenyl)-cyclohexane (alkyl=propyl, pentyl, heptyl) and *trans*-4-n-pentyl-(4'-cyanobiphenyl-4)-cyclohexane (Fig. 2.1) purchased from Merck.

~ EBBA (N-(p-EthoxyBenzylidene)-p'-n-ButylAniline) (Fig. 2.2) synthesized according to a reference book [1] by Ray Syvitski

~ a mixture 55 wt% ZLI-1132/EBBA called '*magic mixture*' a nematic phase that has zero external electric field gradient (*efg*) at approximately 301.4 K [2,3] prepared from pure liquid crystals

The solutes 1,3,5-trichlorobenzene (TCB), 3,5-dichlorotoluene (DCT), 5-chloro m-xylene (CLMX) and mesytilene (MESIT) (Fig. 2.3) were commercially available except 3,5-dichlorotoluene, which was donated by Scott Kroeker from the University of Manitoba. All liquid crystals and solutes were used with no further purification.

3,5-dichlorotoluene, 5-chloro m-xylene and mesytilene were dissolved in liquid crystal solvents in about ~5% mol concentration in 5 mm outer diameter NMR tubes. In each sample ~1% mol concentration of TCB was added as an internal orientational standard for scaling purposes. The mixtures were then heated to the isotropic phase and mixed thoroughly on a vortex stirrer repeatedly until samples became homogeneous.

The NMR tubes were equipped with a capillary tube filled with acetone-d₆, centered in the middle using teflon spacers. The acetone-d₆ was used as a deuterium lock (signal).

Experiment

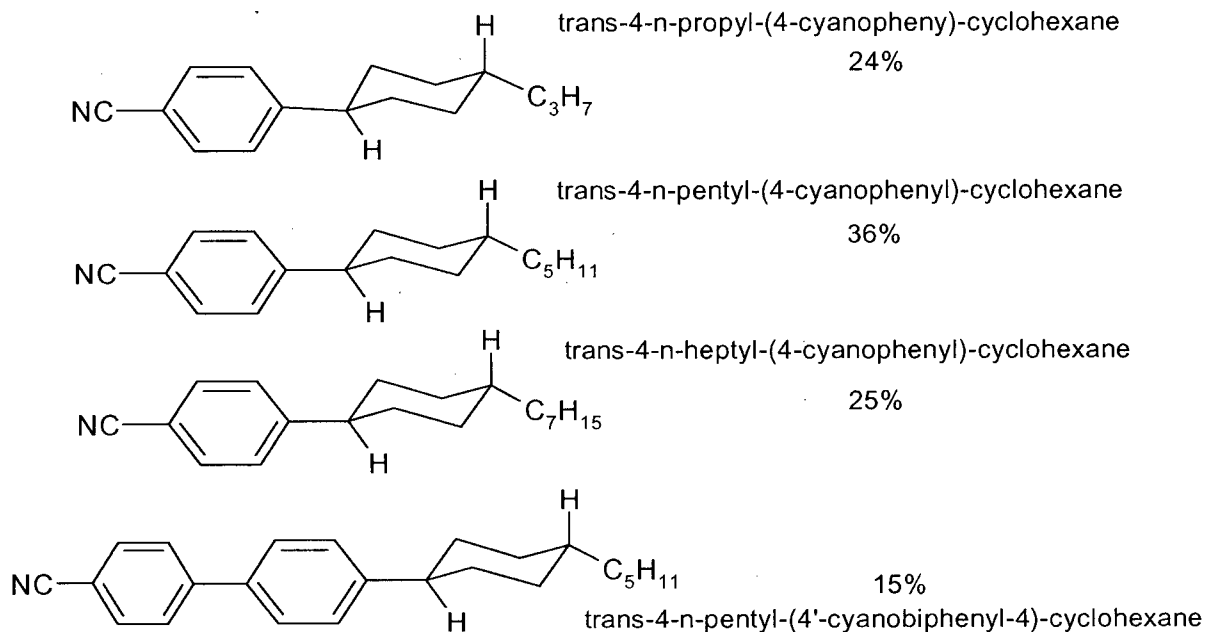


Figure 2.1. ZLI 1132 liquid crystal

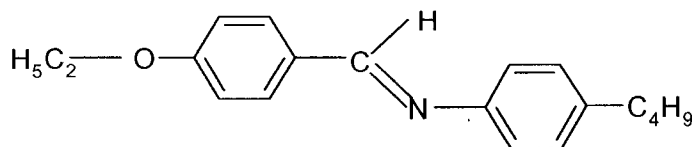


Figure 2.2 EBBA liquid crystal (N-(p-EthoxyBenzylidene)-p'-n-ButylAniline)

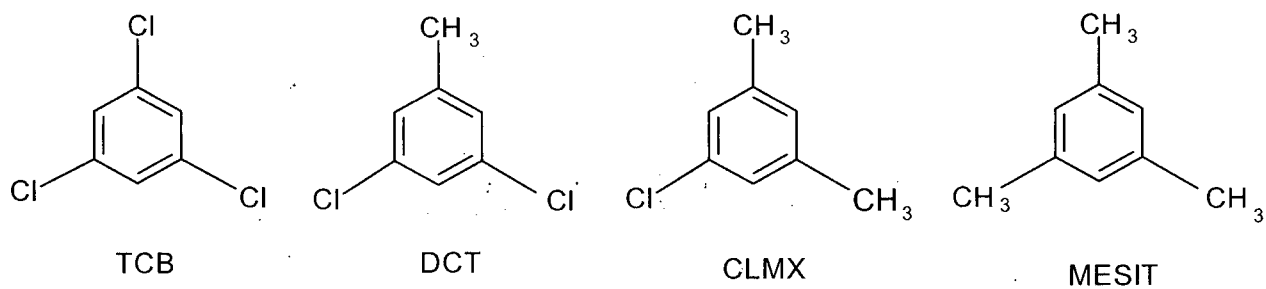


Figure 2.3 Solutes

2.2 EXPERIMENTAL CONDITIONS

Proton high-resolution and multiple-quantum NMR experiments were performed on a Bruker AMX-500 spectrometer equipped with a high resolution probe operating at 11.75 T (corresponding to a proton resonance frequency of 500 MHz). The temperature in the probe was calibrated using the difference in the proton chemical shifts of 80% Ethylene-Glycol/DiMethylSulfOxide-d6 and it was controlled by a Bruker temperature unit using air-flow. The dial temperature of 300.7 K was calibrated to 300.0 K \pm 0.1 K.

All samples were heated up to the isotropic phase and vortexed thoroughly before placing in the NMR probe. They were let to sit in the probe for half an hour in order for them to reach equilibrium. High-resolution proton NMR spectra were acquired using a simple one pulse sequence (Fig. 2.4) with 32K data points that are zero filled to 64K points in the t_2 dimension. The phase of the pulse (ϕ) and the receiver (θ) were cycled according to the cycling scheme in Fig. 2.4 in order to reduce the effects of pulse and receiver imperfections. The 90° degree pulse width varied between 11 μ s and 13 μ s; recycle delay was 2 s; spectral width varied from 13 kHz to 20 kHz depending on the sample, and the number of scans was 100.

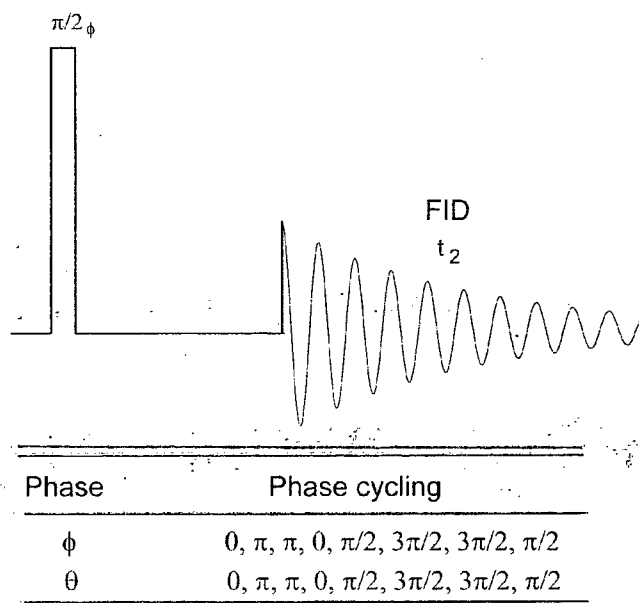


Figure 2.4 Single pulse sequence

Experiment

All multiple quantum (MQ) spectra were acquired simultaneously as separate slices of a three-dimensional spectrum using the 3D MQ-NMR pulse sequence (Fig. 2.5) [4].

MQ coherences excited by the second pulse evolve in variable time t_1 and are converted into observable one-quantum coherences by the third pulse. Individual echoes $S(t_2)$ are acquired as a function of time t_1 and phase ϕ that is incremented by $360^\circ/n$ (n is an arbitrary integer that should be at least $2N+1$) n times for each t_1 value. This gives rise to a 3D interferogram where the signal is a three-dimensional function $S(t_1, \phi, t_2)$.

After Fourier transformation with respect to t_1 , ϕ and t_2 for each value of FT-ed ϕ dimension the MQ spectrum was extracted as the summed projection of the Fourier transforms of the echo signal $S(t_2)$ onto the t_1 dimension.

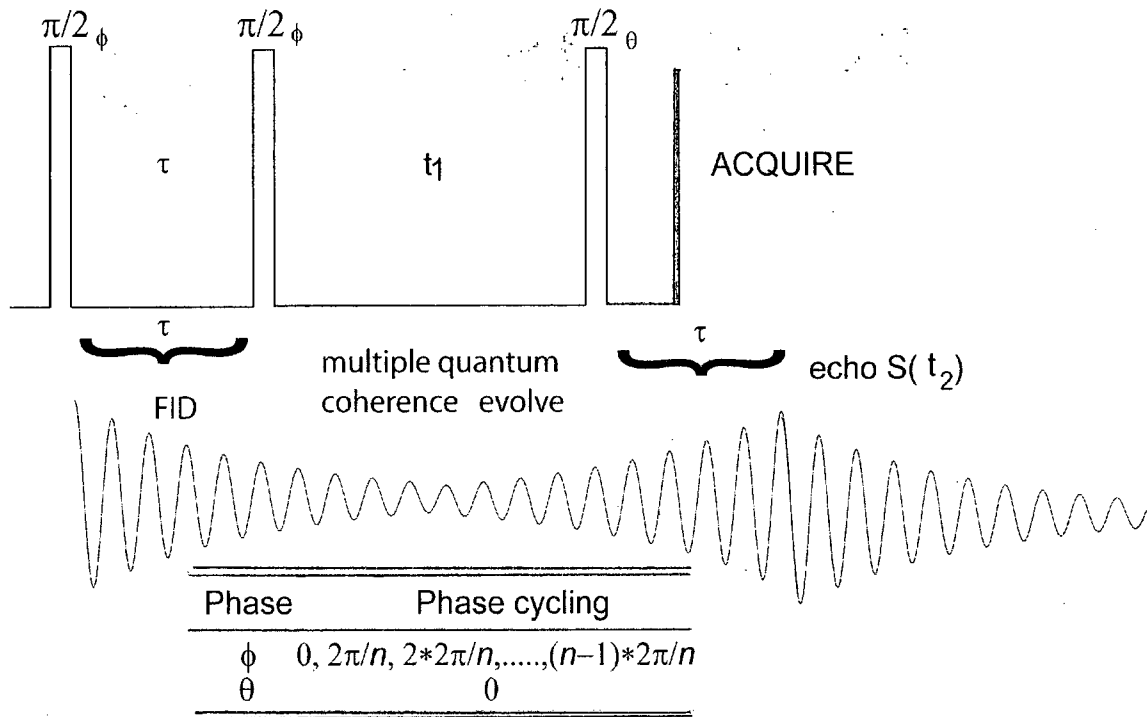


Figure 2.5 3D MQ NMR pulse sequence

Experiment

The experiment time varied between 9 hours for DCT (6 spin) and 36 hours for MESIT (12 spin system). Recycle delays were in the range between 1.3 s and 2 s; preparation τ time ranged between 9 ms and 12 ms (it was chosen so as to produce visible intensities of higher MQ coherences).

In both the t_1 and t_2 dimensions, 1024 points were acquired and zero filled to 2048 points. In the ϕ dimension 16 points (a multiple of 2) for DCT and 32 for CLMX and MESIT were collected.

In order to get rid of coherent noise, the processing parameter FCOR was set to 1 (default value was 0.5 [5]). The FCOR parameter defines that the first point in the real FID was multiplied with its value in order to overcome the rolling baseline caused by the non-simultaneous acquisition of the real and the imaginary signals. In high-resolution experiments the rolling baseline is annulled by setting FCOR to 0.5. On the other hand FCOR=0.5 creates a systematic coherent noise in the 3D MQ experiment.

References:

- [1] Keller, P. and Liebert, L. (1978), *Solid State Phys. Supplemental*, **14**, 19.
- [2] Barker, P.B, Van der Est, A.J., Burnell, E.E., Patey, G.N., de Lange, C.A. and Snijders, J.G., 1984, *Chem. Phys. Lett.*, **107**, 426.
- [3] Van der Est, A.J., Barker, P.B., Burnell, E.E, de Lange, C.A. and Snijders, J.G., 1985, *Mol. Phys.*, **56**, 161.
- [4] Syvitski, R.T., Burlinson, N., Burnell, E.E and Jeener.J., 2002, *J. Magn. Res.*, **155**,251.
- [5] *XWIN-NMR Software Manual*, Bruker Analytik GmbH, 2000.

3. SPECTRAL ANALYSIS

3.1 INTRODUCTION

The NMR experiment for ordered systems provides valuable and precise information such as dipole-dipole and spin-spin interactions, anisotropies in chemical shifts and quadrupole coupling constants. From dipolar couplings, information about relative molecular geometries and conformations as well as second rank order parameters can be easily extracted (Eq. 1.11, page 8).

This chapter explains how spectral parameters were extracted from complex high-resolution proton NMR spectra of small solutes with the help of MQ NMR, as well as how spectral parameters are used to obtain the solute molecular geometry and its second rank orientational order parameters. Those orientational order parameters are important information that will be used later to examine which mechanisms of ordering are dominant in liquid crystal systems.

3.2 SPECTRAL ANALYSIS WITH THE AID OF MQ NMR

High-resolution spectra of small solutes dissolved in liquid crystal solvents are determined by the spin Hamiltonian (equivalent to the Hamiltonian in section 1.5.1):

$$\hat{H} = -\sum_i \nu_i I_{i,z} + \sum_i \sum_{j>i} [(J_{ij} + 2D_{ij}) I_{i,z} I_{j,z} + \frac{1}{2}(J_{ij} - D_{ij})(I_i^+ I_j^- + I_i^- I_j^+)] \quad (3.1)$$

where I^+ and I^- are raising and lowering spin operators, ν_i is the resonance frequency of nucleus i ; and J_{ij} and D_{ij} are the indirect and dipolar coupling constant between nuclei i and j in the molecule. The eigenstates and eigenvalues that govern spectral frequencies and intensities can be calculated from diagonalization of the Hamiltonian for a given set of spectral parameters. Therefore an initial set of spectral parameters is needed to simulate the experimental spectrum.

Spectral analysis

One way of choosing an appropriate initial set of parameters for a molecule is the choosing a set for the same liquid crystal solvent from a molecule with similar size and shape. This approach is only successful in a small number of simple cases (like low-spin symmetrical systems). For more complicated cases (Fig. 3.1) MQ spectra were analyzed first. Due to the poor resolution of MQ spectra (up to 100 Hz) the obtained set of spectral parameters is rather imprecise but it serves as a good starting point for analysis of the high-resolution spectra (where observed line widths were of the order of a few Hz) (see Table 3.2).

Using the initial set of spectral parameters a trial spectrum was calculated. Calculated frequencies were then assigned to the experimental ones using cursor control in the graphical program called SM [1] with macros written by Ray Syvitski and spectral parameters were adjusted in a least-square fitting routine. Assignment and reassignment of frequencies and adjustment of spectral parameters were repeated until a reasonable fit was achieved (a fit that is of the order of the digital resolution of the experimental spectra). During the assignment process non-resolvable and low intensity spectral lines were assigned last to avoid a misleading and meaningless fit. The program used to calculate spectra and iteratively adjust spectral parameters was LEQUOR [2] for high-resolution spectral analysis and its modified version for MQ analysis [3].

Spectral analysis

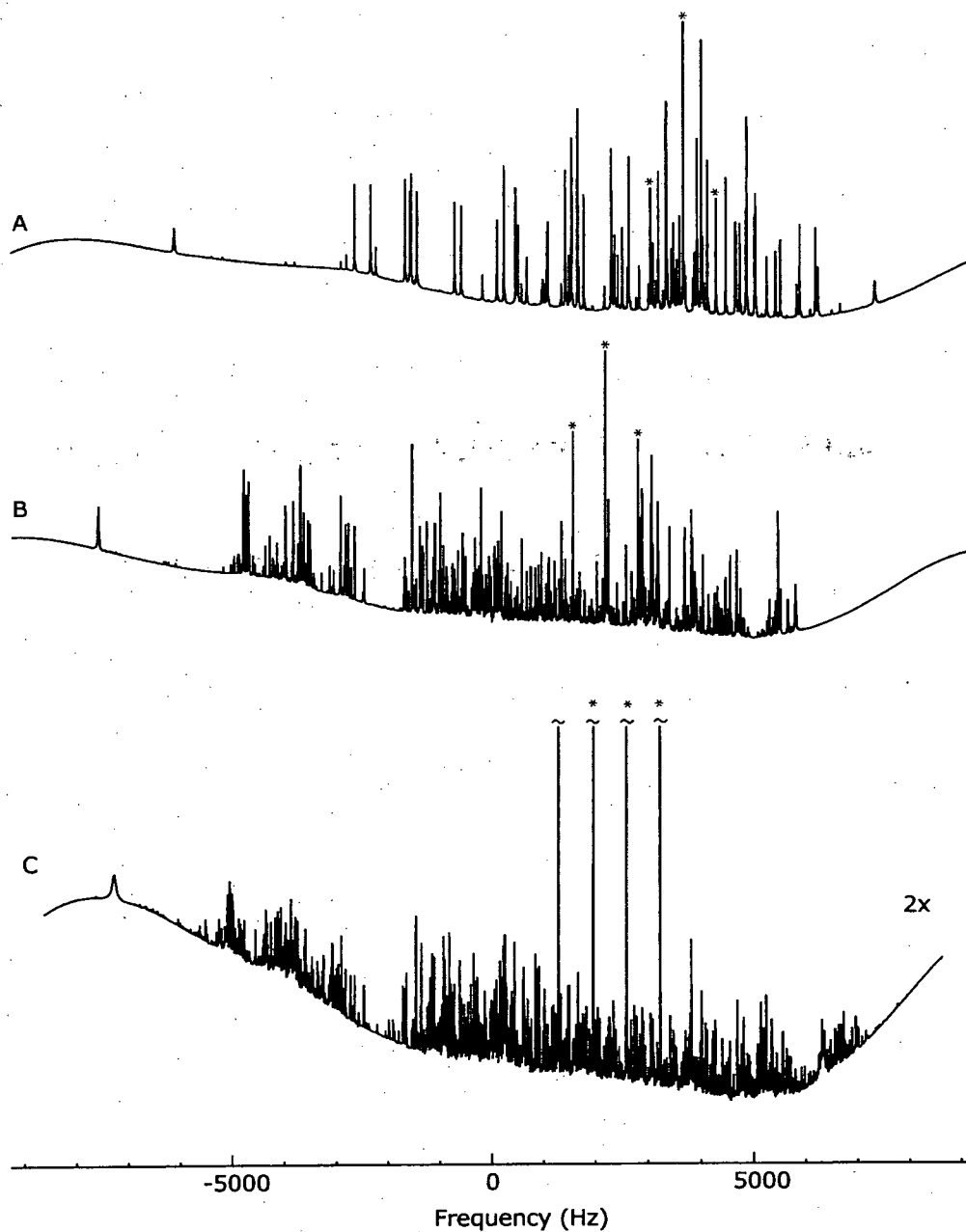


Figure 3.1 High-resolution proton NMR spectra of DCT (A), CLMX (B) and MESIT (C) in ZLI 1132 liquid crystal at 300 K with total number of calculated spectral lines of 69, 782 and 3819. Spectral lines marked with an (*) belong to the internal standard TCB. The rolling baseline is the unresolved spectrum of the ZLI 1132 liquid crystal.

The high-resolution spectrum of TCB (3-spin system) is a 1:2:1 triplet with a splitting of $3 \cdot D_{HH}$ and chemical shift that corresponds to the position of the middle peak (Table 3.1).

Table 3.1 Fitting Parameters and RMS Errors from Analysis of High-Resolution Spectra of TCB 3-spin System

Solutes	Parameter ^a	<u>Liquid Crystal</u>		
		ZLI 1132	55 wt% 1132/EBBA	EBBA
TCB with DCT	D_{HH}	-199.68(01)	-171.92(02)	-138.19(03)
	σ_H^b	3536.85(02)	1875.15(04)	3920.67(06)
	RMS error	0.020	0.045	0.064
TCB with CLMX	D_{HH}	-208.27(04)	-163.52(04)	-144.15(05)
	σ_H^b	2187.67(09)	2590.95(10)	3783.51(11)
	RMS error	0.095	0.099	0.113
TCB with MESIT	D_{HH}	-212.13(04)	-167.65(00)	-144.14(02)
	σ_H^b	2586.97(10)	2528.62(00)	2740.47(05)
	RMS error	0.097	0.001	0.051

^a Parameter in Hz

^b Frequency is referenced to an arbitrary zero. Spectra were acquired at 500.13 MHz.

Determination of spectral parameters of DCT (6-spin system) is a challenging task since DCT has 3 different chemical shifts and 5 independent dipolar coupling constants. In this case an initial set of spectral parameters was obtained from the (N-1) and (N-2)Q spectra (Fig. 3.2). First the (N-1)Q spectrum was fitted using a modified version of the program LEQUOR that allows either independent adjustment of S_{ij} and/or D_{ij} within the fitting

routine. Knowing the geometry of the molecule and the relation between S_{ij} and D_{ij} (Eq. 1.11), by adjusting the S_{ij} , D_{ij} is adjusted automatically. In some cases varying order parameters is an advantage since a smaller number of parameters are fitted to and therefore the spectral analysis is simplified. In the case of the +5Q spectrum of DCT, instead of fitting to 5 independent dipolar coupling parameters only two independent order parameters (S_{zz} and S_{xx} - order parameters in the plane of the benzene ring (Fig. 3.6)) were adjusted within the fitting routine. Since the geometry of DCT hasn't been determined previously, the known geometry of TCB a molecule with similar size and shape, taken from ref. [4] was used as an initial geometry needed to calculate independent D_{ij} parameters. The +5Q and +4Q spectra were easily fitted (Fig. 3.3 and Fig. 3.4) with a RMS error of 4 Hz and the set of spectral parameters obtained (Table 3.2) were then used to simulate the high-resolution spectrum. A total of 68 lines were assigned in the high-resolution spectrum of DCT in EBBA with a RMS error of 0.343 Hz. The fitted high-resolution spectrum is shown in Fig. 3.5 and fitting parameters are presented in Table 3.3. In the calculated spectrum a Lorentzian line broadening of 2 Hz was used to incorporate the natural line broadening effect due to motion and collision in the system.

Similar spectral strategy was applied in solving the high-resolution spectra of CLMX and MESIT molecules. Fitted spectral parameters of those molecules are presented in Tables 3.4 and 3.5.

Table 3.2 Fitting Parameters and RMS Errors from Analysis of MQ and High-Resolution Spectra of DCT in EBBA

Parameter ^a	EBBA	EBBA	EBBA
	+5Q spectrum	+4Q spectrum	+1Q spectrum
D_{12}	- 120.94	- 123.95	-126.39(17)
D_{13}	- 153.60	- 157.74	-157.90(17)
D_{14}	- 399.42	- 396.10	-394.60(08)
D_{34}	- 63.18	- 63.15	-63.58(043)
D_{45}	1161.58	1174.49	1173.95(08)
σ_1 ^b	3861.57	3831.77	3836.03(20)
σ_3 ^b	3913.77	3882.17	3891.44(23)
σ_4 ^b	1686.31	1706.67	1710.42(15)
RMS error (Hz)	3.092	4.094	0.343
Number of assigned lines	6	14	70

^a Parameter in Hz

^b Frequency is referenced to an arbitrary zero. Spectra were acquired at 500.13 MHz.

Spectral analysis

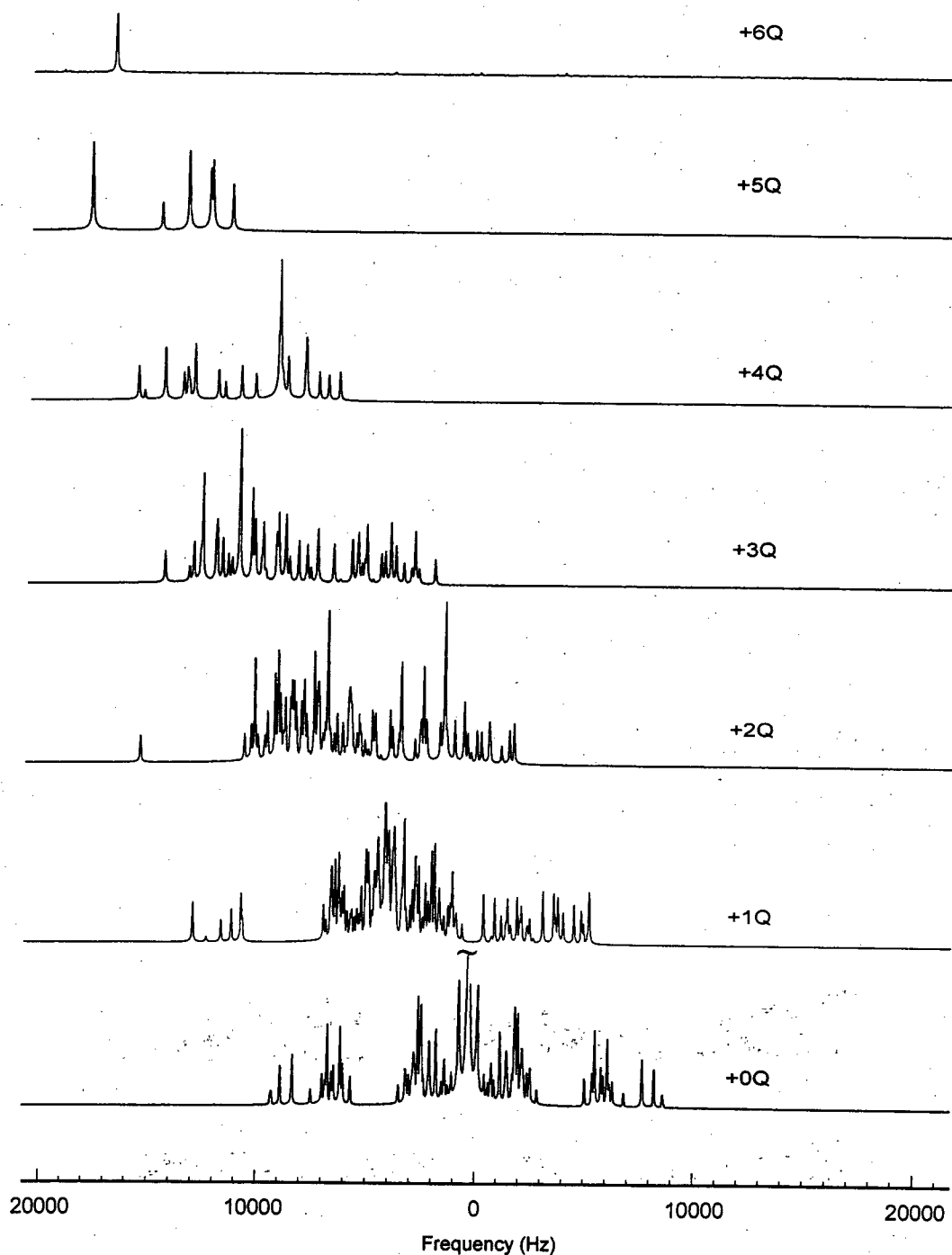


Figure 3.2 All positive MQ spectra of DCT (6-spin system) in EBBA liquid crystal at 300 K. With $\tau = 12$ ms, recycle delay of 2 s, two scans for each $n=16$ phase increments per t_1 , 1024 t_1 increments, F_2 spectral width of 25 kHz and F_1 spectral width of 50 kHz. The +0Q spectrum strong central line was cut off for clarity

Spectral analysis

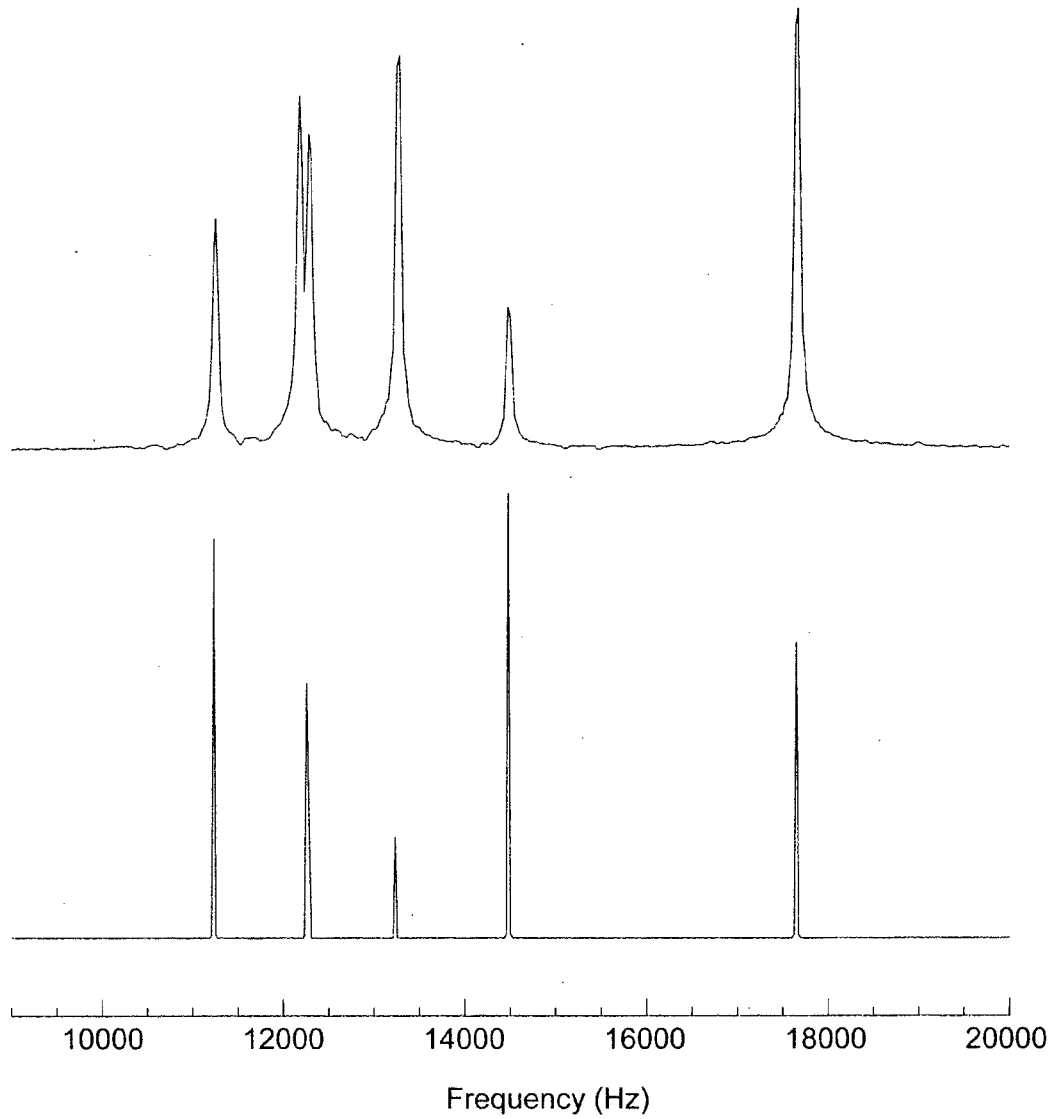


Figure 3.3 Experimental (top) and calculated (bottom) +5Q spectra of DCT in EBBA
Line width in the experimental spectrum is approximately 80 Hz. Two lines around 12000 Hz
in calculated spectrum are not visible separated. The intensities of the calculated spectrum
do not correspond with those of the experimental spectrum

Spectral analysis

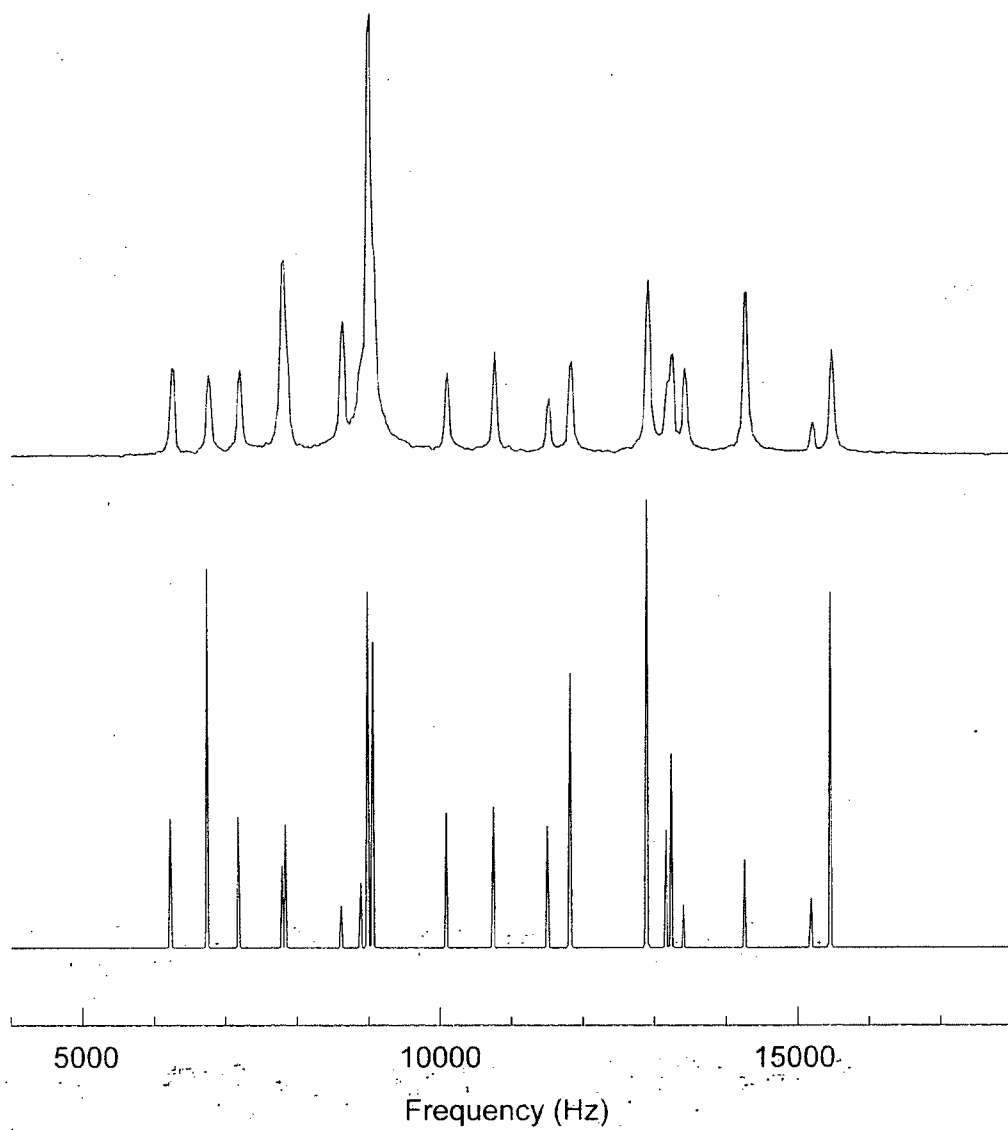


Figure 3.4 Experimental (top) and calculated (bottom) +4Q spectra of DCT in EBBA
Line width in the experimental spectrum is approximately 70 Hz and the intensities of
the calculated spectrum do not correspond with those of the experimental spectrum

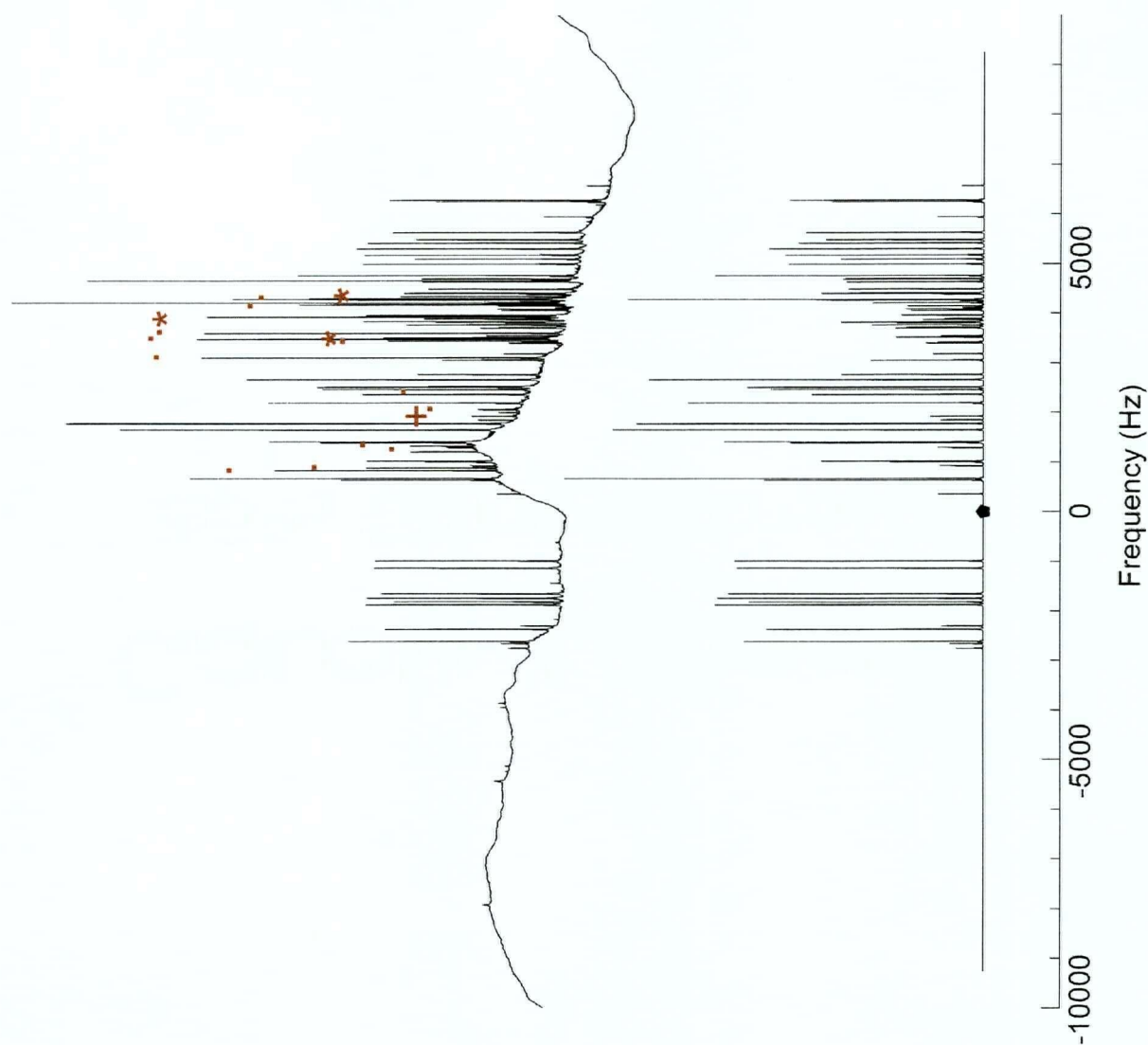
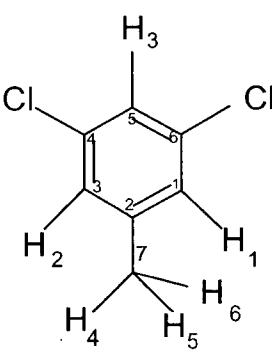


Figure 3.5 Experimental (top) and calculated (bottom) high-resolution proton spectra of DCT in EBBA at 300 K. Spectral lines marked with an (*) belong to the internal standard TCB and resonances marked with an (-) are from unknown impurities (the DCT solute is an old sample that has probably degraded a little bit over a long period of time); less intense resonances (+) belong to the lock solvent (acetone- d_6 in a capillary tube); the rolling base line is the unresolved spectrum of EBBA liquid crystal. In the experimental spectrum the line width at half-maximum height varied between 2-8 Hz. Lorentzian line broadening used in the calculated spectrum is 2 Hz. The intensities of the calculated spectrum closely correspond with those of the experimental spectrum.

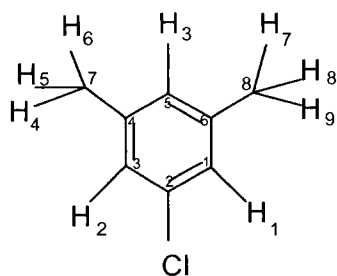
Table 3.3 Fitting Parameters and RMS Errors from Analysis of High-Resolution Spectra of DCT 6-spin System

Solute	Parameter ^a	Liquid Crystal		
		ZLI 1132	55 wt% 1132/EBBA	EBBA
	D_{12}	-255.66(19)	-201.31(19)	-126.39(17)
	D_{13}	-176.15(21)	-162.89(21)	-157.90(17)
	D_{14}	-493.48(08)	-440.10(08)	-394.60(09)
	D_{34}	-56.26(36)	-56.39(36)	-63.58(44)
	D_{44}	1030.85(08)	1039.46(09)	1173.95(08)
	J_{12}^b	-	-	-
	J_{13}	2.06(44)	1.85(40)	2.20(32)
	J_{14}	-0.70(14)	-0.95(14)	-0.72(17)
	J_{34}	-0.38(65)	-0.85(69)	-0.50(84)
	σ_1	3569.70(21)	1862.77(23)	3836.03(20)
	σ_3	3411.09(24)	1787.45(27)	3891.44(73)
	σ_4	1534.72(15)	-266.03(16)	1710.41(15)
	RMS error	0.327	0.546	0.343
	Number of assigned lines	68	61	70

^a Parameter in Hz^b J_{12} coupling constant was not determined due to insensitivity of the fitting process^c Frequency is referenced to an arbitrary zero. Spectra were acquired at 500.13 MHz.

Table 3.4 Fitting Parameters and RMS Errors from Analysis of High-Resolution Spectra of CLMX 9-spin System

Solute	Parameter ^a	<u>Liquid Crystal</u>		
		ZLI 1132	55 wt% 1132/EBBA	EBBA
CLMX	D_{12}	-160.34(11)	-144.20(10)	-167.69(09)
	D_{14}	-70.42(05)	-59.49(07)	-61.95(09)
	D_{17}	-659.22(05)	-495.41(07)	-403.10(07)
	D_{34}	-414.89(07)	-374.65(08)	-439.08(06)
	D_{45}	1292.43(03)	1089.89(03)	1141.24(03)
	D_{47}	-60.26(03)	-54.35(03)	-63.74(03)
	J_{12}	1.99(18)	1.97(18)	2.01(18)
	J_{13}	1.53(10)	1.75(13)	1.37(15)
	J_{14}	-0.51(10)	-0.43(14)	-0.78(17)
	J_{17}	-0.66(11)	-0.69(16)	-0.53(17)
	J_{34}	-0.75(13)	-0.76(17)	-0.77(14)
	J_{47}	-0.18(06)	-0.22(06)	-0.21(06)
	σ_1	2099.63(09)	2497.30(10)	3675.27(10)
	σ_3	2214.41(12)	2546.08(13)	3657.00(13)
	σ_4	91.23(05)	422.84(06)	1578.88(06)
	RMS error	0.560	0.401	0.453
	Number of assigned lines	445	396	379

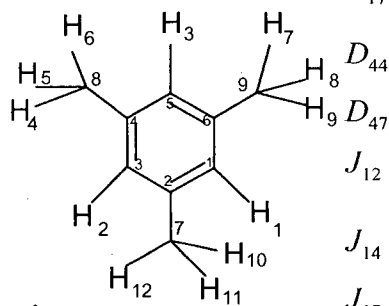


^a Parameter in Hz

^b Frequency is referenced to an arbitrary zero. Spectra were acquired at 500.13 MHz.

Table 3.5 Fitting Parameters and RMS Errors from Analysis of High-Resolution Spectra of MESIT 12-spin System

Solute	Parameter ^a	Liquid Crystal		
		ZLI 1132	55 wt% 1132/EBBA	EBBA
MESIT	D_{12}	-220.49(06)	-179.26(06)	-168.75(06)
	D_{14}	-571.94(03)	-465.51(03)	-439.58(03)
	D_{17}	-82.99(06)	-67.583(07)	-63.79(07)
	D_{44}	1518.15(02)	1234.96(03)	1166.50(03)
	D_{47}	-82.97(02)	-67.53(02)	-63.82(02)
	J_{12}	1.72(11)	1.57(13)	1.76(12)
	J_{14}	-0.71(05)	-0.66(07)	-0.67(07)
	J_{17}	-0.44(10)	-0.41(01)	-0.45(14)
	J_{47}	-0.22(04)	-0.19(05)	-0.22(05)
	σ_1	2510.77(08)	2420.58(10)	2592.37(09)
	σ_4	492.02(05)	367.53(07)	537.91(06)
	RMS error	0.474	0.341	0.371
	Number of assigned lines	494	355	381



^a Parameter in Hz

^b Frequency is referenced to an arbitrary zero. Spectra were acquired at 500.13 MHz.

3.3 MOLECULAR STRUCTURE AND ORDER PARAMETERS

The relative positions of nuclei and order parameters for a given solute were calculated from a simultaneous fit to the dipolar couplings obtained for all three liquid crystals. For this purpose a slightly modified version of a program called SHAPE [3] was used. The program calculates the dipolar couplings according to Eq. 1.11 using initial inputted geometry and it performs the least-square minimization routine NL2SNO [5] that minimizes the difference between calculated and experimentally determined dipolar couplings (which are part of the input data). The exact geometry of solutes used in this study, except TCB, hasn't been measured yet so the initial geometry used in the fitting routine was chosen to be geometry of the molecule with similar size and shape (such as TCB (ref. [4])).

For molecules with rotating groups, such as a methyl group, dipolar interactions must be averaged over a whole rotation. Each methyl group was modeled with a potential function

$$V = V_6(1 - \cos 6\alpha)/2 \quad (3.2)$$

where V_6 is fixed at 60 J/mol [6]. The potential minimum corresponds to the position of the proton in a methyl group that is perpendicular to the benzene ring.

Each methyl group is rotated independently through 360° in 10° steps. For each position dipolar couplings between hydrogens were calculated and averaged over all possible conformations, with each conformation weighted by the Boltzman factor ($\sim e^{-V/kT}$).

As a result of the minimization routine, relative structural parameters and order parameters of the studied solutes DCT, CLM and MESIT were successfully determined and are presented in Tables 3.6 and 3.7. Order parameters were determined with high accuracy. That is quite important since the values of the order parameters of a solute may be quite small and the prime goal of this study is to explore various models for the anisotropic potential.

Spectral analysis

Table 3.6 Structural Parameters from Fits to Dipolar Couplings for DCT, CLMX and MESIT ^a

Parameter ^a	TCB ^d	DCT ^e	CLMX ^e	MESIT ^e
$r(C_1 - C_2)$	1.3908	1.3920(05)	1.3870(19)	1.3861(37)
$r(C_3 - C_4)$	1.3908	1.3898(08)	1.3922(20)	1.3861(37)
$r(C_4 - C_5)$	1.3908	1.3890 ^g	1.3919 ^g	1.3861(37)
$r(C_1 - H)$	1.0940	1.0893(14)	1.0865(24)	1.0881(18)
$r(C_5 - H)$	1.0940	1.0914(14)	1.0903(25)	1.0881(18)
$r(C_2 - X^c)$	1.7326	1.5283(18)	1.7326 ^f	1.5267(27)
$r(C_4 - X^b)$	1.7326	1.7326 ^f	1.5218(30)	1.5267(27)
$r(C - H)_{methyl}$	-	1.0997(13)	1.1114(19)	1.1056(22)
$r(C_6 - C_{methyl})$	-	1.7326 ^f	1.5281(30)	1.5267(27)
$\angle(C_1C_2C_3)$	122.00	121.77 ^g	121.98 ^g	121.64(14)
$\angle(C_2C_3C_4)$	118.00	118.01(07)	118.22(12)	118.36(14)
$\angle(C_3C_4C_5)$	122.00	122.21(15)	121.72(12)	121.64(14)
$\angle(C_4C_5C_6)$	118.00	117.78 ^g	118.13 ^g	118.36(14)
$\angle(C_5C_6X^b)$	121.00	119.00 ^f	118.90(12)	119.18(07)
$\angle(C_4C_3H)$	121.00	120.77(05)	121.35(13)	120.82 ^g
$\angle(C_4C_5H)$	121.00	121.11 ^g	120.93 ^g	120.82 ^g
$\angle(C_1C_2X^a)$	119.00	119.11(05)	119.01(12)	119.18(07)
$\angle(C_6C_{methyl}H_{methyl})$	-	110.47(07)	111.22(16)	110.94(14)
RMS error	-	0.321	0.548	0.566

Spectral analysis

- ^a See figure 3.6 for structure and atom labeling of molecules. Bond distances are in (Å); bond angles in degrees and errors are in Hz
- ^b X=Cl for TCB and CLMX ; X=CH₃ for DCT and MESIT
- ^c X=Cl for TCB and DCT ; X=CH₃ for CLMX and MESIT
- ^d Geometry taken from Ref. [4]
- ^e Initial a priori geometries are TCB geometries taken from Ref. [4]
- ^f Parameter not varied during fit
- ^g Parameter calculated from the bond angles and lengths of the carbon skeleton

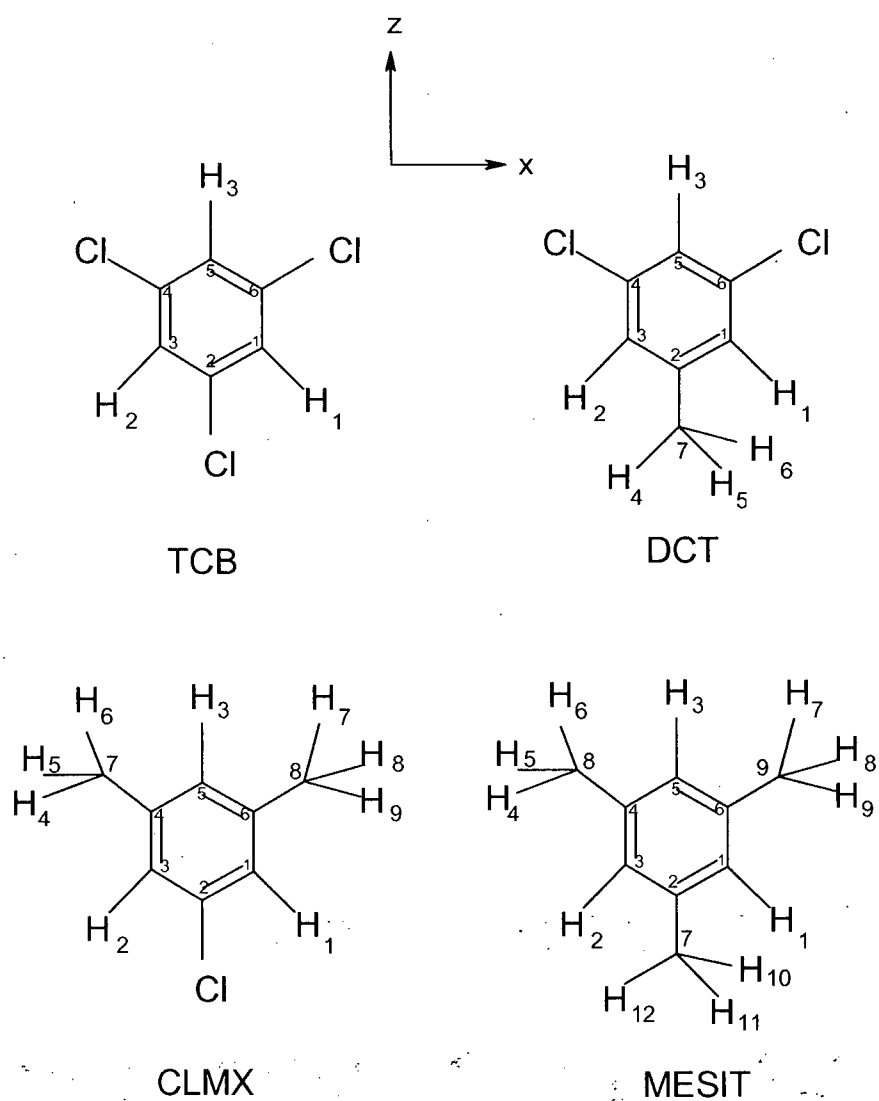


Figure 3.6 Atom labeling of solute molecules

Table 3.7 Table of Order Parameters from Fits to Dipolar Couplings

Solute	Order Parameter ⁺	<i>Liquid Crystal</i>		
		1132	55wt% 1132/EBBA	EBBA
TCB/DCT [~]	S_{xx}	0.13480(01)	0.11606(01)	0.09329(02)
	S_{yy}^*	-0.26960(01)	-0.23212(03)	-0.18658(04)
	S_{zz}	0.13480(01)	0.11606(01)	0.09329(02)
TCB/CLMX [~]	S_{xx}	0.14060(03)	0.11039(03)	0.09731(03)
	S_{yy}^*	-0.28120(05)	-0.22078(05)	-0.19462(05)
	S_{zz}	0.14060(03)	0.11039(03)	0.09731(03)
TCB/MESIT [~]	S_{xx}	0.14321(00)	0.11318(00)	0.09731(01)
	S_{yy}^*	-0.28641(00)	-0.22635(00)	-0.19462(03)
	S_{zz}	0.14321(00)	0.11318(00)	0.09731(01)
DCT	S_{xx}	0.17265(80)	0.13162(50)	0.08347(50)
	S_{yy}^*	-0.27022(11)	-0.23001(82)	-0.19459(86)
	S_{zz}	0.09757(31)	0.09838(32)	0.11112(36)
CLMX	S_{xx}	0.10627(40)	0.09565(35)	0.11186(39)
	S_{yy}^*	-0.28468(03)	-0.22793(83)	-0.21573(79)
	S_{zz}	0.17841(63)	0.13228(48)	0.10387(40)
MESIT [~]	S_{xx}	0.14467(66)	0.11770(54)	0.11117(51)
	S_{yy}^*	-0.28935(32)	-0.23541(08)	-0.22234(02)
	S_{zz}	0.14467(66)	0.11770(54)	0.11117(51)

^{*} Order parameter that is perpendicular to the benzene ring

$$^+ S_{xx} + S_{yy} + S_{zz} = 0$$

$$^~ S_{xx} = S_{zz}$$

3.4 SUMMARY

In this study spectral, structural and orientational order parameters for TCB, DCT, CLMX and MESIT dissolved in three different liquid crystals were determined. An initial set of spectral parameters, used in the analysis of the high-resolution spectrum, was estimated from the analysis of the (N-1) and (N-2)Q spectra adjusting either S_{ij} or D_{ij} independently. With this approach analysis was simplified and therefore analysis time was significantly reduced. Highly accurate spectral parameters were extracted by analyzing the high-resolution spectrum. Accurate order parameters and relative positions of nuclei were obtained by simultaneously fitting to all dipolar coupling parameters of the solute in all liquid crystals.

References:

- [1] Graphical Interface program SM, Edition 2.2.0. Jan. 1992, Lupton, R. and Monger, P.
- [2] Diehl, P., Kellerhals, H. and Niederberger, W., 1971, *J. Magn. Resonance*, **4**, 352.
- [3] Syvitski, R. and Burnell, E.E., 2000, *J. Chem. Phys.*, **113**, 3452.
- [4] Almenninbgen, A. and Hargittai, I., 1984, *J. Mol. Struct.*, **116**, 119.
- [5] Dennis, J. E., Gay, D. M. and Welsch, R. E., 1981, *ACM Trans. Math. Software*, **7**, 3.
- [6] Lister, D., MacDonald, J. and Owen, N., 1978, *Internal Rotation and Inversion*, Academic Press, London.

4. ORIENTATIONAL ORDERING IN NEMATIC LIQUID CRYSTALS

Investigation of different contributions to the orientational mechanisms in nematic liquid crystals

4.1 INTRODUCTION

Previous studies on orientational mechanisms in nematic liquid crystals gave great insight into the nature of the physical interactions responsible for orientational behaviour in these phases. Generally they show that the main orientational ordering mechanism comes from short-range interactions [1-7], *i.e.* the repulsive interactions that are closely correlated with the size, shape and flexibility of the molecules. Contributions from the long-range interactions, interactions that are due to properties that describe the distribution of the charge over a molecule (like dipole, quadrupole, polarizability) seem to have a less dominant effect on the orientational ordering [8-11]. To what extent each electrostatic long-range interaction contributes to the orientational mechanisms is still an open debate.

The purpose of this study is to determine the effects of permanent dipoles, quadrupoles and molecular polarizabilities on orientational ordering. In order to reduce the effect of dominant short-range interactions and to emphasize different electrostatic interactions, solutes with similar size and shape but different electrostatic properties are chosen as probe solutes in various liquid crystals.

The set of chosen solutes with similar size and shape (Fig. 4.1) have either C2 or C3 type symmetry. If they had the same size and shape and if the size and shape is the only orientational mechanism then the anisotropy of the experimentally determined order parameters ($S_{xx} - S_{zz}$) would be zero due the same symmetry. And if any other orientational mechanisms beside size and shape also contributes to the orientational ordering then the anisotropy in the order parameters would be influenced by them, and they should differ from zero. Particularly the anisotropy in the order parameters in the magic mixture (zero electric field gradient and quadrupole interaction) will allow the clear manifestation of dipole and polarizability effects.

Comparing the anisotropy of the experimentally determined order parameters ($S_{xx} - S_{zz}$) in a series of solutes with the same size and shape but different electrostatic properties, a qualitative picture about long-range electrostatic contributions to the orientational mechanisms can be drawn. It should be stressed that behind this way of examining the experimental results is the assumption that all solutes have the same size and shape. A more quantitative approach to learning about intermolecular interactions is to compare the experimental order parameters with calculated order parameters from theory or models, or those determined from computer simulations. As described in the introductory chapter two short-range potential (Cl and size and shape) models and three long-range potential (dipole, quadruple and polarizability) models were utilized to investigate the orientational mechanism in nematic liquid crystals.

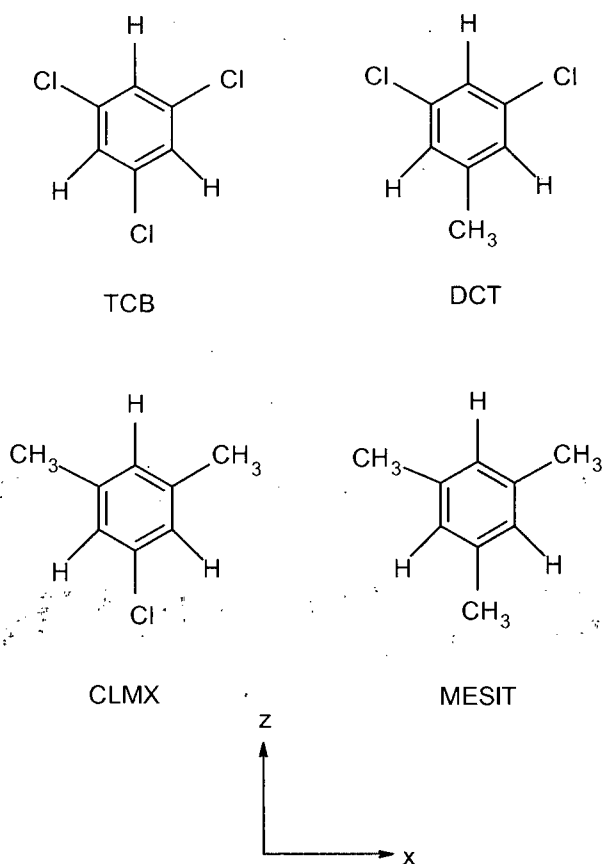


Figure 4.1 Chosen set of solutes with the same size and shape but different electrostatic properties presented in their coordinate system

4.2 DETERMINATION OF A CONSISTENT SET OF ORDER PARAMETERS

When solutes are dissolved in liquid crystal solvents they tend to slightly perturb the liquid crystal environment. The perturbation effect depends on solute properties and solute concentration in a given sample.

If one needs to compare the solute orientational order parameters in different samples then all the above mentioned factors must be compensated for. In other words a consistent set of order parameters must be obtained. That can be done in a few different ways [1,7,11-13].

For example, spectra can be recorded at the same reduced temperature ($T_R = \frac{T}{T_{NI}}$, where

T_{NI} is the nematic-to-isotropic phase transition temperature) or order parameters of each solute in the liquid crystal can be measured as a function of concentration and then extrapolated to zero concentration.

In the present study a constant real temperature scaling approach, shown to give the most consistent results, [13] is utilized. Order parameters were scaled using the internal standard TCB and the simple equation:

$$S_{ij(solute)}^{scaled} = \frac{S_{ij(solute)}}{S_{ij(TCB)}} \cdot S_{ij(TCB-reference)} \quad (4.1)$$

where $S_{ij(solute)}$ and $S_{ij(TCB)}$ are the order parameters of the solute and internal standard TCB in the same sample tube and $S_{ij(TCB-reference)}$ is the order parameter of internal standard TCB used as a reference tube (arbitrarily chosen to be TCB with MESIT sample tube) in the same liquid crystal.

The set of scaled and non-scaled order parameters is presented in Table 4.1. Differences between scaled and non-scaled values of order parameters of different solutes (DCT, CLMX and MESIT) in the same liquid crystal are less than 6 % using this scaling method (see Fig. 4.2). Also comparing scaled and non-scaled values of order parameters of TCB coodissolved with various solutes for the same liquid crystal the discrepancies are less than 6% (Table

Orientational ordering in nematic liquid crystals

3.7). Both discrepancies imply that the main contribution to the difference comes from solute properties since the concentration of solutes is very small and roughly the same.

Table 4.1 Scaled and Non-Scaled Order Parameters

Solute	Scaled/ Non-scaled Order Parameter *	<i>Liquid Crystal</i>		
		1132	55wt% 1132/EBBA	EBBA
TCB †	S_{xx}^{scaled} / S_{xx}	0.14321/0.14321	0.11318/0.11318	0.09731/0.09731
	S_{yy}^{scaled} / S_{yy}	-0.28642/-0.28642	-0.22636/-0.22636	-0.19462/-0.19462
	S_{zz}^{scaled} / S_{zz}	0.14321/0.14321	0.11318/0.11318	0.09731/0.09731
DCT	S_{xx}^{scaled} / S_{xx}	0.18342/0.17265	0.12835/0.13162	0.08707/0.08347
	S_{yy}^{scaled} / S_{yy}	-0.28707/-0.27022	-0.22429/-0.23000	-0.20297/-0.19459
	S_{zz}^{scaled} / S_{zz}	0.10365/0.09757	0.09594/0.09838	0.11590/0.11112
CLMX	S_{xx}^{scaled} / S_{xx}	0.10824/0.10627	0.09807/0.09565	0.11185/0.11186
	S_{yy}^{scaled} / S_{yy}	-0.28996/-0.28468	-0.23369/-0.22793	-0.21572/-0.21572
	S_{zz}^{scaled} / S_{zz}	0.18172/0.17841	0.13562/0.13228	0.10387/0.10387
MESIT	S_{xx}^{scaled} / S_{xx}	0.14467/0.14467	0.11770/0.11770	0.11117/0.11117
	S_{yy}^{scaled} / S_{yy}	-0.28934/-0.28934	-0.23540/-0.23540	-0.22234/-0.22234
	S_{zz}^{scaled} / S_{zz}	0.14467/0.14467	0.11770/0.11770	0.11117/0.11117

* Order parameters were scaled to order parameters of internal standard TCB in the sample of TCB with MESIT for each liquid crystal

† TCB codissolved with MESIT sample

Orientational ordering in nematic liquid crystal

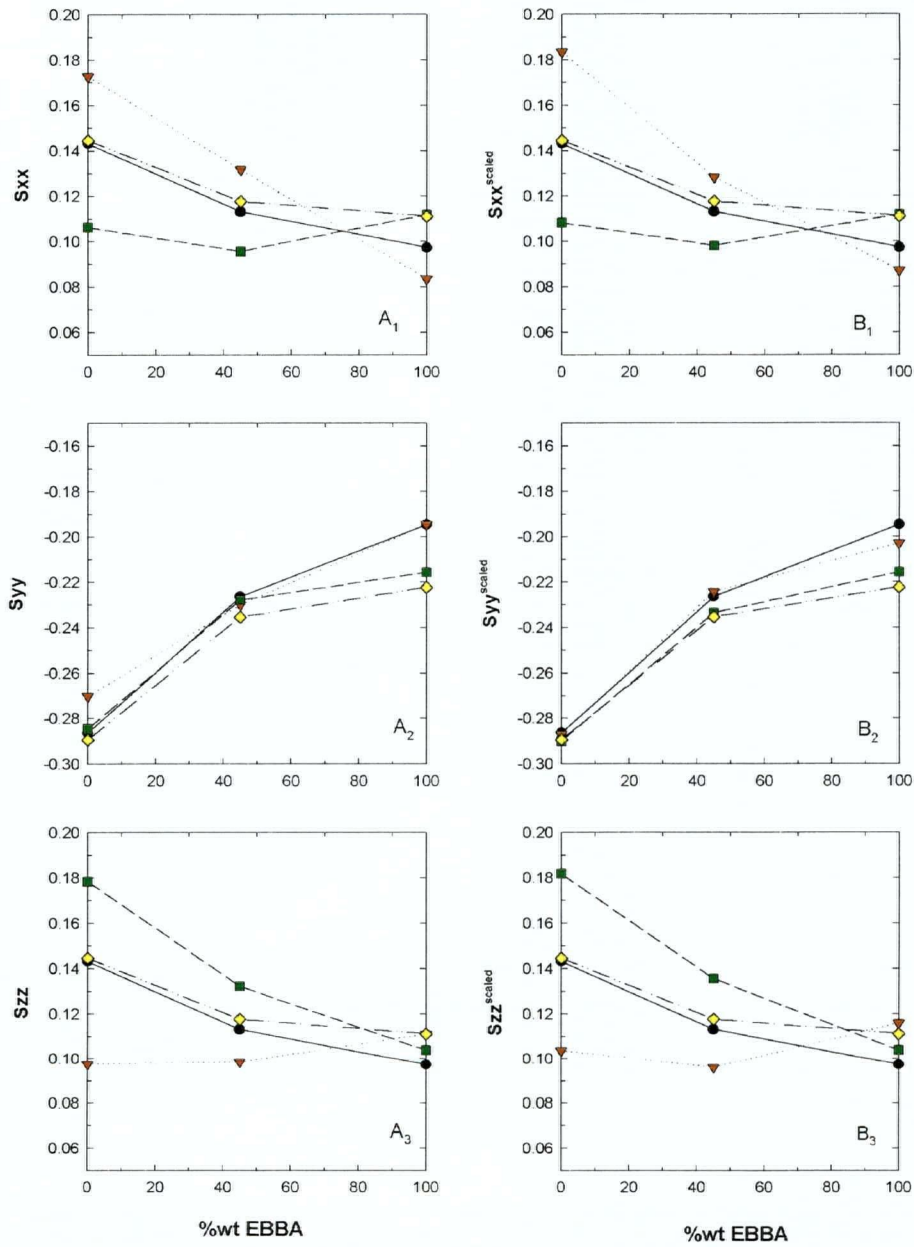


Figure 4.2 Non-scaled (series A) and scaled (series B) experimental order parameters

/ taken from Table 4.1 /

● TCB ▼ DCT ■ CLMX ◆ MESIT

4.3 QUALITATIVE COMPARISON BETWEEN EXPERIMENTAL ORDER PARAMETERS

An intuitive picture about electrostatic interactions that are a consequence of the electrostatic distribution in the molecules can be obtained by examining the relationships between experimental order parameter (or their anisotropies) and molecular properties (or their anisotropies). Starting with the relationship between order parameters with potential Eq. 1.16 (page 13) and long-range potentials with molecular properties Eq. 1.20-22 (page 16-17) , a connection between order parameter and molecular properties can be derived. For the dipole potential model that correlation presented in the simplified fashion (in the high-temperature limit)* :

$$S_{xx} - S_{zz} \propto \frac{U_{Dipole}^{LR}}{kT} \propto -(\mu_{xx}^2 - \mu_{zz}^2) \langle \bar{R}_{zz} - \bar{R}_{xx} \rangle \quad (4.2)$$

If the dipole interaction is important in the orientation then from Eq. 4.2 the order parameter anisotropy would behave linearly with the anisotropy of the squared dipole moment. For the two polar molecules DCT and CLMX the anisotropies of the squared dipole moment (see Table 4.3) have the same sign but the anisotropies in their order parameters have opposite sign (Table 4.2 or Fig. 4.3). This seems to indicate that dipoles do not play a role in the orientation of these solutes in the liquid crystals.

In the magic mixture it is expected that only dipole and polarizability effects can be seen. Since dipoles are of no importance let's see if there is a correlation between polarizabilities (their anisotropies) and anisotropies in the order matrix. Following the same rationale as for dipoles, the polarizability (anisotropy) correlation with order parameter anisotropy should be linear with appropriate sign if polarizability has an effect on the orientation:

$$S_{xx} - S_{zz} \propto \frac{U_{Polarizability}^{LR}}{kT} \propto -(\alpha_{xx} - \alpha_{zz}) \langle \bar{E}_{zz}^2 - \bar{E}_{xx}^2 \rangle \quad (4.3)$$

* In the high temperature limit potential energy is much smaller than thermal energy kT , so the exponential function can be expanded and truncated at the first non-zero term as $e^{-x} \approx 1 - x$.

The anisotropies in the polarizabilities for DCT ($\alpha_{xx} - \alpha_{zz} = 1.922 \cdot 10^{-40} \text{ Cm}^2 / \text{V}$) and CLMX ($\alpha_{xx} - \alpha_{zz} = -1.457 \cdot 10^{-40} \text{ Cm}^2 / \text{V}$) (taken from Table 4.3) are similar, with opposite signs and they linearly follow the anisotropies in the order parameters (Table 4.2 or Fig. 4.3), *i.e.* the anisotropies in the order parameters also have opposite signs, implying that polarizability may have an important role in the orientational ordering of the solutes.

Table 4.2 Anisotropy in Scaled and Non-Scaled Order Parameters

Solute	Anisotropy in Scaled and Non-Scaled Order Parameters *	Liquid Crystal		
		1132	55wt% 1132/EBBA	EBBA
TCB ⁺	$S_{xx}^{scaled} - S_{zz}^{scaled}$	0.00000	0.00000	0.00000
	$S_{xx} - S_{zz}$	0.00000	0.00000	0.00000
DCT	$S_{xx}^{scaled} - S_{zz}^{scaled}$	0.07977	0.03241	-0.02883
	$S_{xx} - S_{zz}$	0.07509	0.03324	-0.02764
CLMX	$S_{xx}^{scaled} - S_{zz}^{scaled}$	-0.07347	-0.03755	0.00799
	$S_{xx} - S_{zz}$	-0.07214	-0.03662	0.00799
MESIT	$S_{xx}^{scaled} - S_{zz}^{scaled}$	0.00000	0.00000	0.00000
	$S_{xx} - S_{zz}$	0.00000	0.00000	0.00000

* Order parameters were scaled to order parameters of internal standard TCB in the sample of TCB with MESIT for each liquid crystal; ⁺ TCB codissolved with MESIT sample

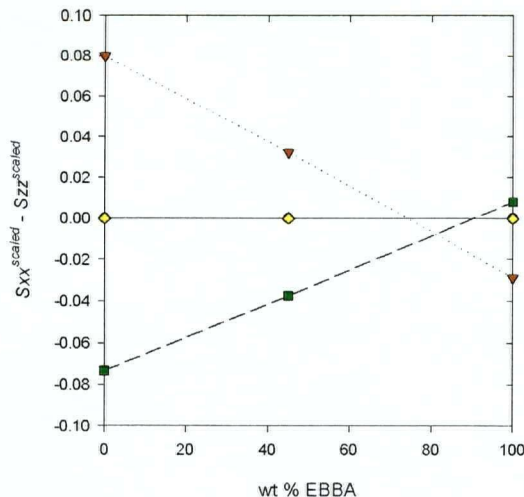


Figure 4.3 Anisotropy in scaled order parameters / values taken from Table 4.2 /
 ▼ DCT ■ CLMX ◆ TCB, MESIT

4.4 COMPARISON BETWEEN EXPERIMENTAL AND THEORETICALLY CALCULATED ORDER PARAMETERS / quantitative approach /

Different combinations of a short-range model (CI or SS) with or without long-range contributions (dipole and/or quadrupole and/or polarizability) were used in a minimization fitting routine. The routine calculates order parameters with Eq. 1.16 (page 13) using various potential functions by performing the non-linear least square fits to experimental order parameters while varying potential parameters.

Potential functions for short- and long-range interactions utilized in the calculation were described earlier in the introductory chapter (Eq. 1.18-22, page 14-17).

Molecular properties such as molecular dipoles, quadrupoles and polarizability factors used in long-range models were calculated with respect to the center of mass using Gaussian 98 [14] with B3LYP/6-311++G** (theory/basis set). Obtained values are reported in Table 4.3. Geometries used in the G98 input file are the geometries obtained from spectral analysis of high-resolution spectra (Table 3.6) which are then converted into the center of mass coordinate system.

Intermolecular potential parameters obtained for various combinations of potential models are presented in Table 4.4.

For the CI potential model the k_{zz} parameter was adjusted while the k_s and k parameters were fixed at $48.0 \cdot 10^{-9} \text{ Jm}^{-2}$ and $2.04 \cdot 10^{-9} \text{ Jm}^{-2}$ (Eq. 1.18). The k_s and k parameters were taken from the NMR study of 46 solute molecules dissolved in 55 wt% 1132/EBBA [1]. For the SS potential model $M_{\alpha\beta}$ (reported in Table 4.4) and k_{zz} parameters were varied independently.

Table 4.3 Molecular Electrostatic Parameters ^a

Solute	Dipole Moment		Quadrupole Tensor			Polarizability Tensor		
	Component ^b		Component ^{c,f}			Component ^{d,g}		
	μ_x ^e	μ_z	Q_{xx}	Q_{yy}	Q_{zz}	α_{xx}	α_{yy}	α_{zz}
TCB	0.025 ^h	-0.017 ^h	0.349 ⁱ	-0.690	0.341 ⁱ	21.634 ⁱ	9.438	21.663 ⁱ
DCT	0.147 ^h	-7.188	-1.555	-1.407	2.962	22.225	10.131	20.303
CLMX	0.011 ^h	7.024	2.418	-1.973	-0.445	20.342	10.909	21.799
MESIT	0.125 ^h	-0.021 ^h	1.139 ⁱ	-2.146	1.007 ⁱ	20.883 ⁱ	11.529	20.515 ⁱ

^a Values calculated with respect to the center of mass using Gaussian 98 with B3LYP/6-311++G** (theory/basis set). Axis labeling is shown in Figure 4.1.

^b Units of $10^{-30} \text{ C} \cdot \text{m}$ ($1 \text{ C} \cdot \text{m} \equiv 2.99793 \cdot 10^{11} \text{ esu}$).

^c Units of $10^{-39} \text{ C} \cdot \text{m}^2$ ($1 \text{ C} \cdot \text{m}^2 \equiv 2.99793 \cdot 10^{13} \text{ esu} \cdot \text{cm}$).

^d Units of $10^{-40} \text{ C} \cdot \text{m}^2 \cdot \text{V}^{-1}$ ($1 \text{ C} \cdot \text{m}^2 \cdot \text{V}^{-1} \equiv 8.9878 \cdot 10^{15} \text{ cm}^3$).

^e For all solutes the μ_y component is zero.

^f For all solutes the Q_{xy} and Q_{yz} components are zero.

^g For all solutes the α_{xy} and α_{yz} components are zero.

^h Values taken as zero (by symmetry) in the fitting routine.

ⁱ Due to a D_{3h} type symmetry, xx and zz tensor components of molecular parameters should be the same. Therefore their averaged values were used in the fitting routine.

Table 4.4 Adjusted Parameters in the Fitting Procedure

a/ CI model combined with/without long-range models

Liquid crystal	CI fitting parameter k_{zz} ^a	Dipole $\langle \bar{R}_{zz} - \bar{R}_{xx} \rangle$ ^b parameter	Quadrupole \bar{F}_{zz} ^c parameter	Polarizability $\langle \bar{E}_{zz}^2 - \bar{E}_{xx}^2 \rangle$ ^d parameter	SS fitting M_{xx} ^a parameter	SS fitting M_{yy} ^a parameter	SS fitting M_{zz} ^a parameter	Error ^f
<u>Fit #1</u>								
1132	1.46 (05)	- ^e	- ^e	- ^e	- ^e	- ^e	- ^e	
MM	0.96 (03)	- ^e	- ^e	- ^e	- ^e	- ^e	- ^e	1.32
EBBA	0.84 (03)	- ^e	- ^e	- ^e	- ^e	- ^e	- ^e	
<u>Fit #2</u>								
1132	1.46 (05)	-2.9 (8.0)	- ^e	- ^e	- ^e	- ^e	- ^e	
MM	0.96 (04)	1.7 (8.5)	- ^e	- ^e	- ^e	- ^e	- ^e	1.29
EBBA	0.83 (03)	8.4 (8.7)	- ^e	- ^e	- ^e	- ^e	- ^e	
<u>Fit #3</u>								
1132	1.48 (03)	- ^e	-2.4 (0.7)	- ^e	- ^e	- ^e	- ^e	
MM	0.96 (02)	- ^e	-0.1(0.7)	- ^e	- ^e	- ^e	- ^e	0.86
EBBA	0.80 (02)	- ^e	4.0 (0.7)	- ^e	- ^e	- ^e	- ^e	
<u>Fit #4</u>								
1132	1.07 (12)	- ^e	- ^e	68.9 (19.9)	- ^e	- ^e	- ^e	
MM	1.02 (11)	- ^e	- ^e	-9.9 (20.4)	- ^e	- ^e	- ^e	0.79
EBBA	1.58 (12)	- ^e	- ^e	-135.3 (21.0)	- ^e	- ^e	- ^e	
<u>Fit #5</u>								
1132	1.48 (04)	1.9 (5.8)	-2.4 (0.7)	- ^e	- ^e	- ^e	- ^e	
MM	0.96 (03)	2.1 (6.2)	-0.1 (0.8)	- ^e	- ^e	- ^e	- ^e	0.86
EBBA	0.80 (02)	0.5 (6.3)	4.0 (0.8)	- ^e	- ^e	- ^e	- ^e	
<u>Fit #6</u>								
1132	1.07 (13)	1.1 (5.3)	- ^e	69.9 (21.5)	- ^e	- ^e	- ^e	
MM	1.01 (12)	1.2 (5.6)	- ^e	8.8 (22.1)	- ^e	- ^e	- ^e	0.79
EBBA	1.57 (13)	1.1 (5.7)	- ^e	-134.4 (22.6)	- ^e	- ^e	- ^e	
<u>Fit #7</u>								
1132	3.18 (61)	- ^e	-11.5 (9.8)	-289.5(103.6)	- ^e	- ^e	- ^e	
MM	2.95 (40)	- ^e	-33.0 (6.7)	-340.5 (69.1)	- ^e	- ^e	- ^e	0.46
EBBA	2.83 (38)	- ^e	-7.1 (2.1)	-348.7 (65.5)	- ^e	- ^e	- ^e	
<u>Fit #8</u>								
1132	3.31 (60)	3.8 (3.1)	-12.5 (3.2)	-312.8(102.2)	- ^e	- ^e	- ^e	
MM	3.03 (40)	4.7 (3.3)	-11.6 (2.2)	-354.6 (67.8)	- ^e	- ^e	- ^e	0.42
EBBA	2.88 (38)	3.5 (3.3)	-7.6 (3.0)	-358.6 (64.6)	- ^e	- ^e	- ^e	

Orientational ordering in nematic liquid crystals

b/ SS model combined with/without long-range models

Liquid crystal	CI fitting parameter k_{zz}^a	Dipole $\langle \bar{R}_{zz} - \bar{R}_{xx} \rangle^b$ parameter	Quadrupole \bar{F}_{zz}^c parameter	Polarizability $\langle \bar{E}_{zz}^2 - \bar{E}_{xx}^2 \rangle^d$ parameter	SS fitting M_{xx}^a parameter	SS fitting M_{yy}^a parameter	SS fitting M_{zz}^a parameter	Error ^f
<u>Fit #9</u>								
1132	1.48 (09)	- ^e	- ^e	- ^e				
MM	1.00	- ^e	- ^e	- ^e	-628 (27)	1257 (56)	-630 (29)	1.62
EBBA	0.89 (06)	- ^e	- ^e	- ^e				
<u>Fit #10</u>								
1132	1.49 (10)	-3.1 (1.3)	- ^e	- ^e				
MM	1.00	1.2 (11.8)	- ^e	- ^e	-628 (27)	1256(60)	-628 (33)	1.60
EBBA	0.88 (06)	7.5 (11.8)	- ^e	- ^e				
<u>Fit #11</u>								
1132	1.51 (04)	- ^e	-6.2 (0.6)	- ^e				
MM	1.00	- ^e	-2.6 (0.6)	- ^e	-643 (12)	1298 (25)	-655 (13)	0.66
EBBA	0.83 (02)	- ^e	1.9 (0.6)	- ^e				
<u>Fit #12</u>								
1132	1.04 (15)	- ^e	- ^e	126.0 (13.1)				
MM	1.00	- ^e	- ^e	44.8 (13.4)	-467 (48)	942 (97)	-475 (49)	0.72
EBBA	1.53 (19)	- ^e	- ^e	-47.2 (13.6)				
<u>Fit #13</u>								
1132	1.51 (04)	-8.6 (5.3)	-6.2 (0.6)	- ^e				
MM	1.00	6.6 (4.9)	-2.7 (0.6)	- ^e	-648 (12)	1294 (26)	-646 (14)	0.61
EBBA	0.83 (02)	4.6 (4.9)	1.9 (0.6)	- ^e				
<u>Fit #14</u>								
1132	1.04 (16)	4.0 (5.3)	- ^e	134.6 (13.7)				
MM	1.00	4.0 (5.5)	- ^e	45.8 (14.1)	-466 (51)	931 (103)	-465 (51)	0.70
EBBA	1.54 (20)	5.6 (6.2)	- ^e	-46.0 (14.1)				
<u>Fit #15</u>								
1132	1.03 (26)	- ^e	-6.9 (2.7)	-19.3 (58.2)				
MM	1.00	- ^e	-7.1 (1.9)	-97.1 (38.4)	-1018 (159)	2058 (320)	-1039 (162)	0.52
EBBA	0.95 (19)	- ^e	-3.3 (1.8)	-110.6 (36.5)				
<u>Fit #16</u>								
1132	1.12 (23)	10.5 (3.8)	-9.1 (2.4)	-63.6 (50.8)				
MM	1.00	10.4 (3.7)	-8.2 (1.7)	-114.5 (33.8)	-1095 (132)	2189 (263)	-1093 (132)	0.40
EBBA	0.94 (16)	8.9 (3.7)	-4.1 (1.5)	-124.8 (30.8)				

Orientational ordering in nematic liquid crystals

c/ long-range models alone and combined

Liquid crystal	CI fitting parameter k_{zz} ^a	Dipole $\langle \bar{R}_{zz} - \bar{R}_{xx} \rangle$ ^b parameter	Quadrupole \bar{F}_{zz} ^c parameter	Polarizability $\langle \bar{E}_{zz}^2 - \bar{E}_{xx}^2 \rangle$ ^d parameter	SS fitting M_{xx} ^a parameter	SS fitting M_{yy} ^a parameter	SS fitting M_{zz} ^a parameter	Error ^f
<u>Fit #17</u>								
1132	- ^e	167.1 (106.9)	- ^e	- ^e	- ^e	- ^e	- ^e	
MM	- ^e	133.5 (108.6)	- ^e	- ^e	- ^e	- ^e	- ^e	16.41
EBBA	- ^e	130.0 (108.8)	- ^e	- ^e	- ^e	- ^e	- ^e	
<u>Fit #18</u>								
1132	- ^e	- ^e	27.3 (9.3)	- ^e	- ^e	- ^e	- ^e	
MM	- ^e	- ^e	23.4 (9.4)	- ^e	- ^e	- ^e	- ^e	13.98
EBBA	- ^e	- ^e	24.5 (9.6)	- ^e	- ^e	- ^e	- ^e	
<u>Fit #19</u>								
1132	- ^e	- ^e	- ^e	246.4 (15.8)	- ^e	- ^e	- ^e	
MM	- ^e	- ^e	- ^e	169.4 (12.1)	- ^e	- ^e	- ^e	2.81
EBBA	- ^e	- ^e	- ^e	146.2 (10.9)	- ^e	- ^e	- ^e	
<u>Fit #20</u>								
1132	- ^e	56.8 (124.0)	25.0 (11.1)	- ^e	- ^e	- ^e	- ^e	
MM	- ^e	36.8 (121.9)	21.8 (11.2)	- ^e	- ^e	- ^e	- ^e	13.89
EBBA	- ^e	31.0 (118.6)	23.2 (11.3)	- ^e	- ^e	- ^e	- ^e	
<u>Fit #21</u>								
1132	- ^e	12.1 (17.4)	- ^e	245.8 (16.2)	- ^e	- ^e	- ^e	
MM	- ^e	12.5 (18.1)	- ^e	168.4 (12.5)	- ^e	- ^e	- ^e	2.72
EBBA	- ^e	18.5 (18.6)	- ^e	144.5 (11.3)	- ^e	- ^e	- ^e	
<u>Fit #22</u>								
1132	- ^e	- ^e	5.6 (1.0)	252.8 (8.5)	- ^e	- ^e	- ^e	
MM	- ^e	- ^e	5.3 (1.0)	166.0 (6.0)	- ^e	- ^e	- ^e	1.22
EBBA	- ^e	- ^e	8.6 (1.0)	137.8 (5.7)	- ^e	- ^e	- ^e	
<u>Fit #23</u>								
1132	- ^e	0.44 (8.2)	5.6 (1.1)	252.8 (9.0)	- ^e	- ^e	- ^e	
MM	- ^e	0.7 (8.7)	5.3 (1.1)	166.0 (6.4)	- ^e	- ^e	- ^e	1.22
EBBA	- ^e	-0.6 (8.9)	8.6 (1.1)	137.8 (6.0)	- ^e	- ^e	- ^e	

^a Units of 10^{-23} J.

^b Units of 10^{36} V / C m^2 .

^c Units of 10^{17} V / m^2 .

^d Units of 10^{17} V² / m^2 .

^e Parameter was not adjusted.

^f Units of 10^{-2} .

A. Short-Range Model Comparison

Examining the difference between S_{xx}^{scaled} and S_{xx}^{calc} order parameters as a function of S_{xx}^{scaled} (Fig. 4.4, Fit #1 and Fit#9) that result from fits to short-range models alone it can be stated that in magic mixture the CI model is excellent (Fig. 4.4, A₂, with errors up to 5-6%) while the SS model is less satisfying (Fig. 4.4, B₂, with errors up to 14%).

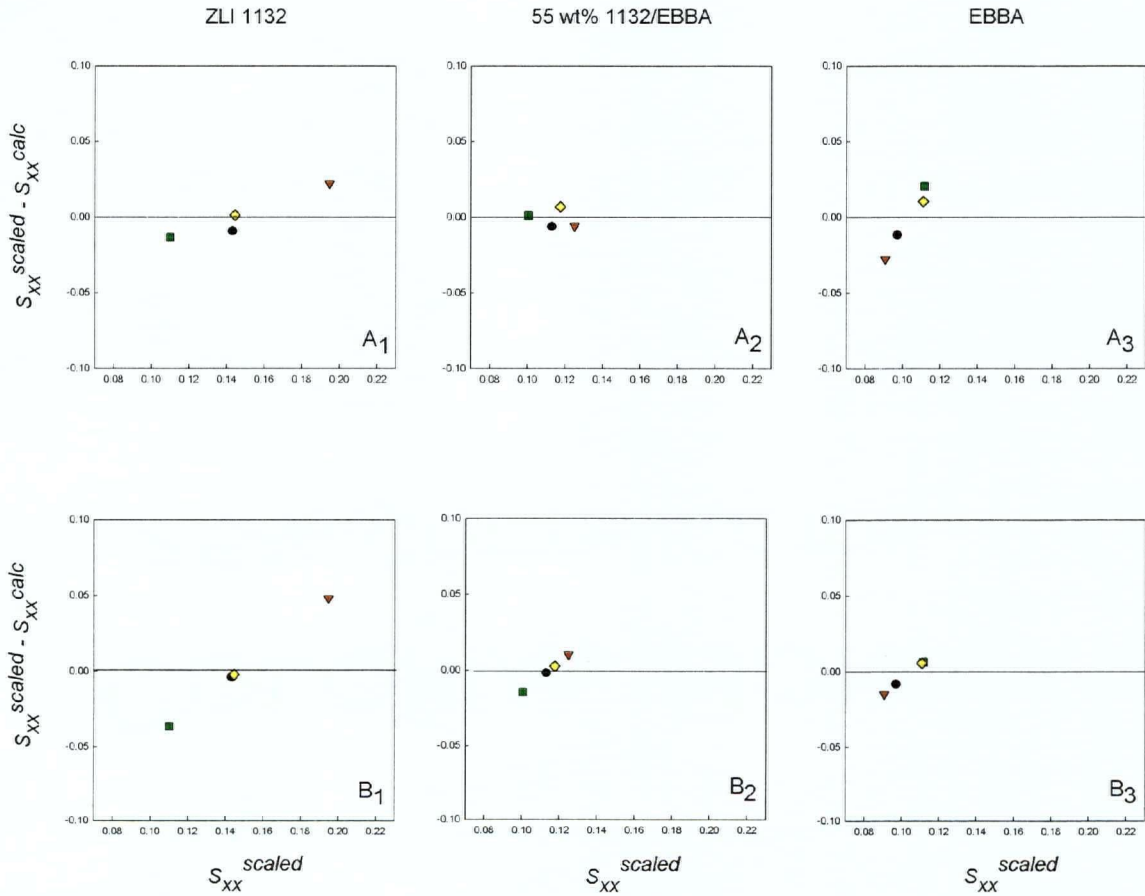


Figure 4.4 Differences between S_{xx}^{scaled} and S_{xx}^{calc} as a function of S_{xx}^{scaled} for short-range models alone. Series A are results from Fit #1(CI model) with $RMS=1.32 \cdot 10^{-2}$ and series B are results from Fit #9(SS model) with $RMS=1.62 \cdot 10^{-2}$.

● TCB ▼ DCT ■ CLMX ◆ MESIT

The CI model uses geometries determined individually for each solute from high-resolution spectral analysis. On the contrary the SS model assumes that all solutes have the same geometry, and it doesn't take into account that DCT and CLMX geometries slightly deviate from D_{3h} symmetry. That could explain why the CI model fits better than the SS model and therefore in the following investigations only the CI model in combination with long-range models will be considered.

Not surprisingly the fits for pure liquid crystals are poorer (Fig. 4.4 A_1 , A_3 , B_1 , B_3) (with discrepancies up to 30%, see DCT in A_3 , or B_1). The same trends are seen for S_{yy}^{scaled} and S_{zz}^{scaled} . This allows for investigation of what other contributions to the short-range interaction might improve the fit and to what extent they might contribute to the orientational mechanism. In that manner of thinking different long-range contributions will be additively combined with short-range ones and their combined contributions will be examined in part C-E.

B. Long-Range Model Comparison

Although short-range models reasonably well describe the orientational mechanism, especially in the magic mixture, let's see what information we can get if we assume that the orientational mechanism can be described with only long-range electrostatic interactions. Judging by the RMS of the Fits #17-19 (Table 4.4) that belong to various electrostatic models alone and by comparing the differences between experimental and calculated order parameters, dipole (Fit #17) alone (Fig. 4.5, series C) and quadrupole (Fit #18) alone (Fig. 4.5, series D) are significantly worse than short-range (Fit #1) (Fig. 4.5, series A). The Fit #19 (Fig. 4.5, series E) that accounts for polarizability effects alone with RMS of $2.81 \cdot 10^{-2}$ is qualitatively and quantitatively better than other long-range fits alone but still worse than short-range fits alone ($RMS(\text{Fit}\#1)=1.32 \cdot 10^{-2}$, $RMS(\text{Fit}\#9)=1.62 \cdot 10^{-2}$).

Almost the same RMS and fitted potential parameters are reached when the Fits #17-19 were repeated *only* for the magic mixture.

The anisotropy in the polarizability tensor is strongly affected by size and shape anisotropy. That connection between polarizability with size and shape is even more stressed by the fact that the polarizability fit alone, although worse than the size and shape model, explains relatively well the experimental results. More about polarizability effects to the

orientational ordering mechanism will be discussed later when comparing short-range with long-range contributions in an additive manner.

Although Fits #22 and #23 (combination of two/three long-range models) show small RMS the fits are meaningless since fitted \overline{F}_{zz} values have very large associated errors due to the large number of adjusting parameters and possible correlation between potential models. Therefore those fits won't be taken into consideration.

Using only magic mixture spectral parameters in the fitting routine where the quadrupole contribution is expected to be zero, the aim was to investigate the effects of other long-range potentials like dipole and polarizability. Fig. 4.6 contains fits of different pairs of short-range with long-range interactions *only* for the magic mixture. Fit F belongs to short-range (CI) model alone, fit G is combination of CI model with dipole model, fit H is CI model with quadrupole model and fit I is CI model with polarizability model. The equality of the Fits A and H indicates that the quadrupole interaction in magic mixture is annulled and that potential parameter $\overline{F}_{zz} \approx 0$. It is also obvious that overall all fits look the same (Fig. 4.6) with the same $\text{RMS} = 0.94 \cdot 10^{-2}$, the same k_{zz} and zero \overline{F}_{zz} , $\langle \overline{R}_{zz} - \overline{R}_{xx} \rangle$ and $\langle \overline{E}_{zz}^2 - \overline{E}_{xx}^2 \rangle$ parameters.

From all of the above, we can say that in magic mixture long-range interactions do not play an important role in the orientational mechanism and that short-range interactions are the only dominant contributor to the orientational ordering.

Orientational ordering in nematic liquid crystal

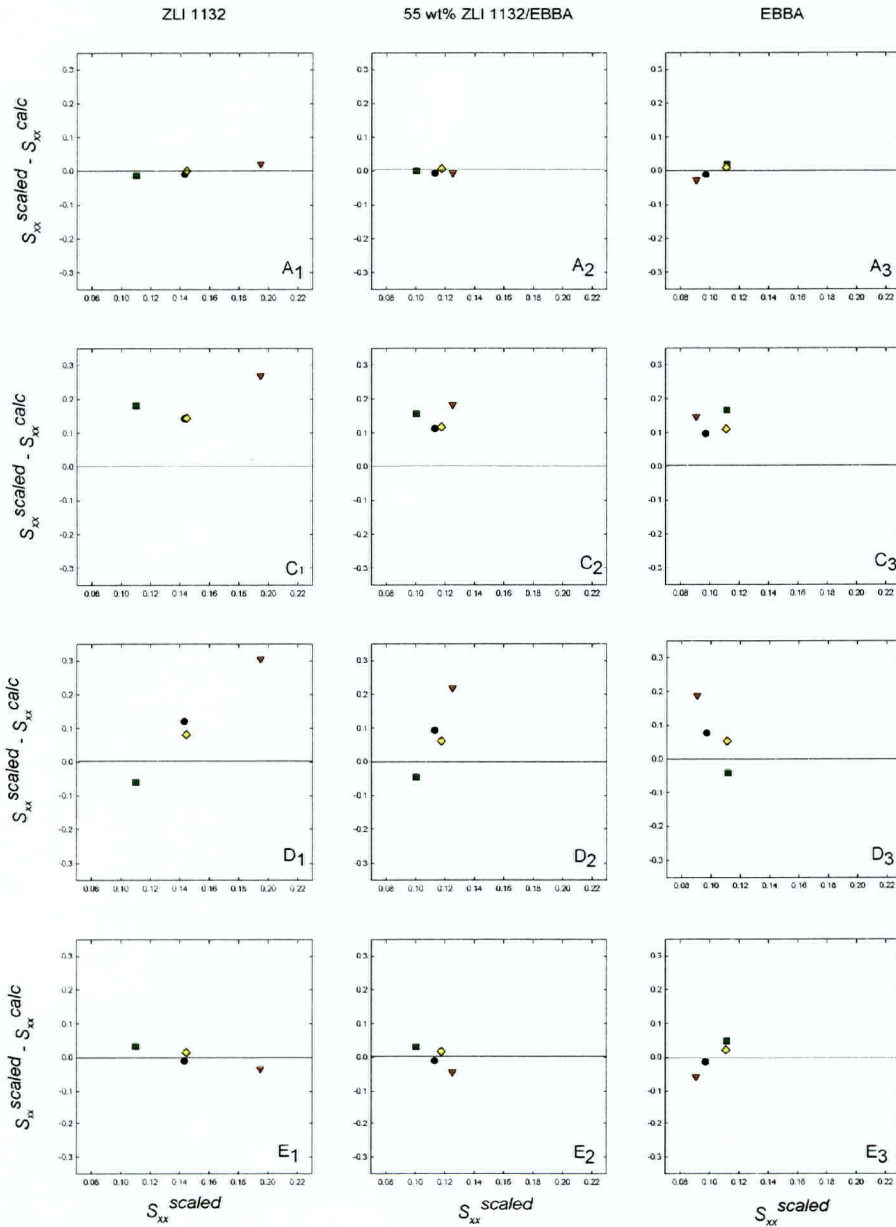


Figure 4.5 Differences between S_{xx}^{scaled} and S_{xx}^{calc} as a function of S_{xx}^{scaled}

Series A are results from Fit #1(CI model) used for comparison; Series C are results from Fit #17 (Dipole model) ; Series D are results from Fit #18 (Quadrupole model); Series E are results from Fit #19 (Polarizability model).

● TCB ▼ DCT ■ CLMX ◆ MESIT

Orientational ordering in nematic liquid crystal

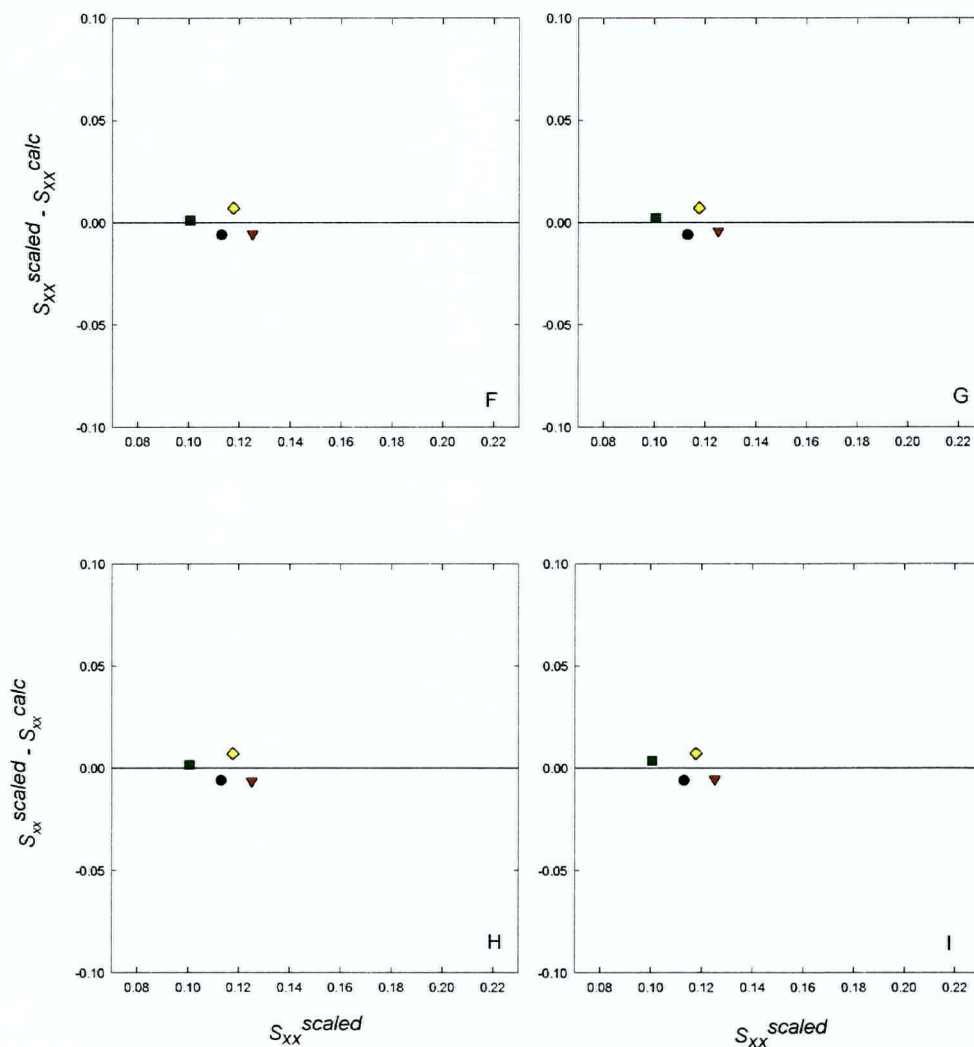


Fig 4.6 Different pairs of short with long-range interaction fits when *only* magic mixture order parameters were used

Fit F is CI model alone, Fit G is CI with Dipole, Fit H is CI with Quadrupole and Fit I is CI with

Polarizability model

● TCB ▼ DCT ■ CLMX ◆ MESIT

C. Dipolar Interaction Contribution

The qualitative picture drawn earlier shows that dipoles have no noticeable effect on the orientation of the solutes. The same conclusion is evident by examining the RMS values (Table 4.4) and Fit #1 (CI model) and Fit #2 (CI+Dipole) or Fit #9 (SS model) and Fit #10 (SS+Dipole)(Fig. 4.7, compares series A with J and/or series B with K) for molecules with dipoles. Both fits with or without dipole contribution are the same, with the same fitting k_{zz} parameters and RMS errors. Also the dipole potential fitted parameters $\langle \bar{R}_{zz} - \bar{R}_{xx} \rangle$ are zero within the calculated errors (see Table 4.4). Within the context of the results, dipoles are not an important factor in the orientation of the solutes (also in agreement with previous studies [15]) and won't be taken into account further.

D. Quadrupolar Interaction Contribution

Previous studies characterized the quadrupolar interaction as an interaction with a significant contribution to the orientational mechanism. Comparing the Fit #1(CI model) with Fit #3 (CI+Quadrupole) and/or Fit #2 (CI+Dipole) with Fit #5 (CI+Dipole+Quadrupole), *i.e* comparing series A with L and/or series M with N shown in Fig. 4.8, the same conclusion follows. The significant drop in RMS between fits with the quadruple contribution as opposed to only short-range contributions implies that this might be attributed to the effect of the quadrupole interaction.

It should also be pointed out that the quadrupole potential parameter \bar{F}_{zz} does change sign from ZLI 1132 to EBBA, being almost zero for the magic mixture 55 wt% 1132/EBBA. The sign obtained for \bar{F}_{zz} in EBBA is positive ($\bar{F}_{zz} = 4.0 \cdot 10^{17} V / Cm^2$) and in 1132 is negative ($\bar{F}_{zz} = -2.4 \cdot 10^{17} V / Cm^2$). This is not consistent with the signs of the electric field gradients in the component liquid crystals determined from molecular hydrogen experiments [16] and mono- and di- substituted benzene molecule experiments [15]. This difference opens a new question that needs to be investigated. Maybe our assumption of using a mean field approach is too simple. Running Monte Carlo simulations (as part of future work) that employs the quadrupole interaction can be used to test the validity of the mean-field

approach, as well as gain a better picture as to what extent the quadrupole interaction contributes to the orientational mechanism.

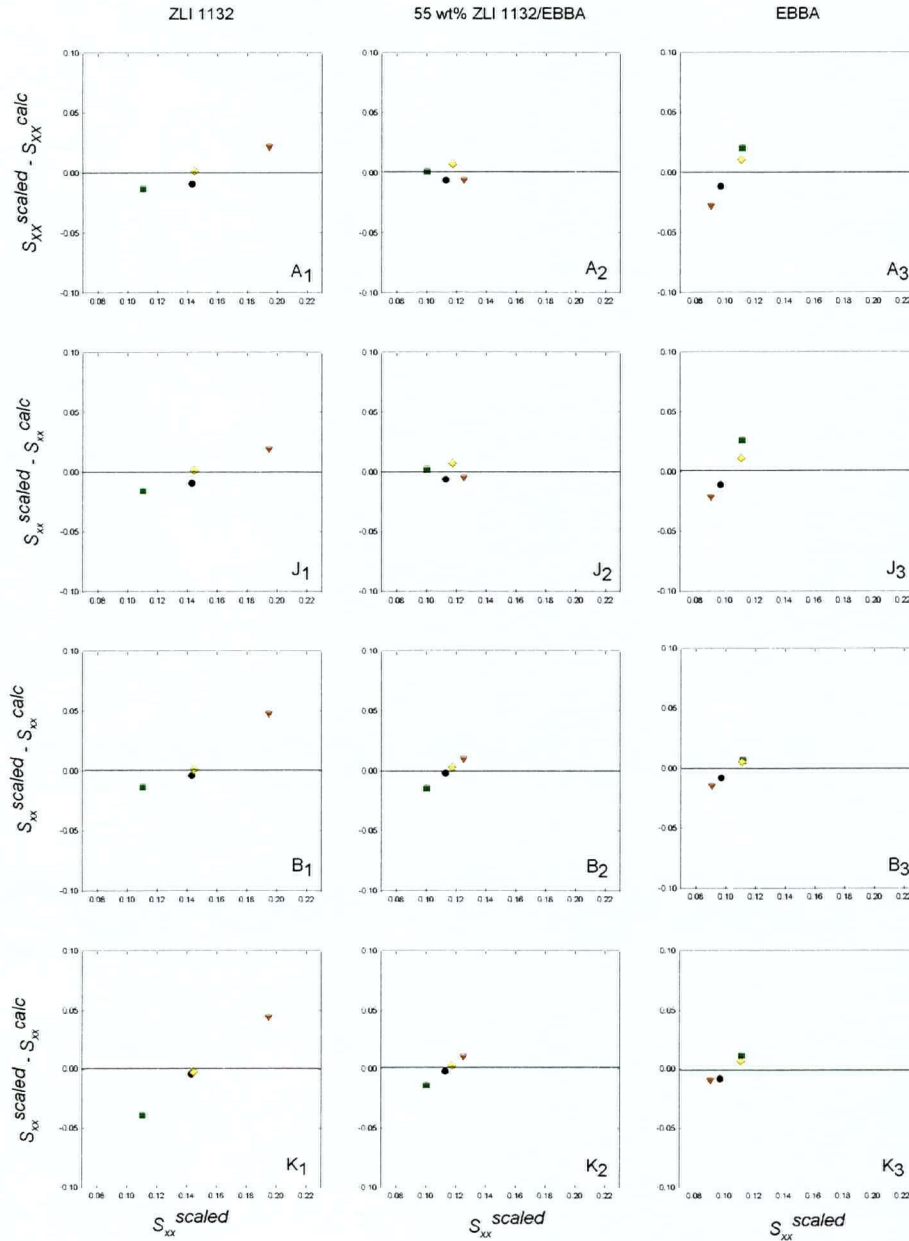


Fig 4.7 Differences between S_{xx}^{scaled} and S_{xx}^{calc} as a function of S_{xx}^{scaled}

Series A and B are results from Fit #1 (CI model) and Fit #9 (SS model);
 Series J and K are results from Fit #2 (CI+Dipole) and Fit #10 (SS+Dipole)

● TCB ▼ DCT ■ CLMX ◆ MESIT

Orientational ordering in nematic liquid crystal

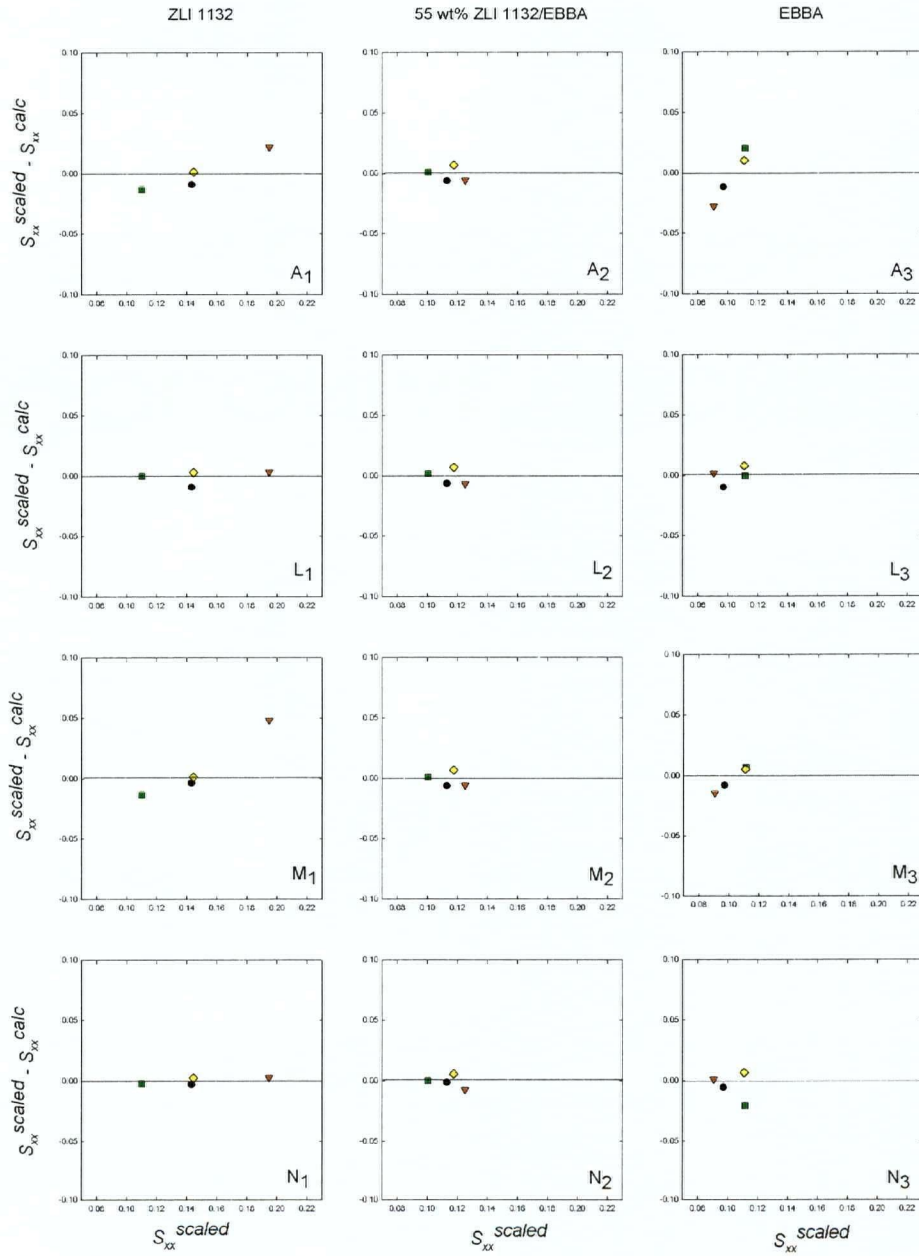


Fig 4.8 Differences between S_{xx}^{scaled} and S_{xx}^{calc} as a function of S_{xx}^{scaled}

Series A and L are results from Fit #1 (CI model) and Fit #3 (CI+Quadrupole);

Series M and N are results from Fit #2 (CI+Dipole) and

Fit #5 (CI+ Dipole+Quadrupole)

● TCB ▼ DCT ■ CLMX ◆ MESIT

Certain Fits (#7, #8, #15, #16) that contain a quadrupole contribution in combination with other long-range interactions are discarded as meaningless, since the potential parameters \bar{F}_{zz} obtained have large calculated errors. The explanation for this finding might be the existence of a correlation between the different potential models. The reason for getting a good RMS in these cases is the fact that by adding another potential more available fitting parameters are introduced into the fitting routine.

E. Polarizability Interaction Contribution

Comparing the RMS errors of Fits #1, #4 and #6 or Fits #9, #12 and #14 significant change is noticed when the polarizability interaction is added to the fitting. This is more obvious when comparing series A (CI model), O (CI with Polarizability) and P (CI with Dipolar and Polarizability model) (see Fig. 4.9). In the magic mixture the polarizability potential parameters $\langle \bar{E}_{zz}^2 - \bar{E}_{xx}^2 \rangle$ are zero within the calculated errors (Table 4.4), once more agreeing with the results found in magic mixture fits (section B, page 59, 61), *i.e.* that in the magic mixture long-range interactions are not affecting the ordering mechanism since the CI short-range model so wonderfully explains the experimental results.

In the component liquid crystals the polarizability model significantly improves the fit. All this indicates that the polarizability effect could be considered as one of the contributors to the orientational ordering mechanism.

Orientational ordering in nematic liquid crystal

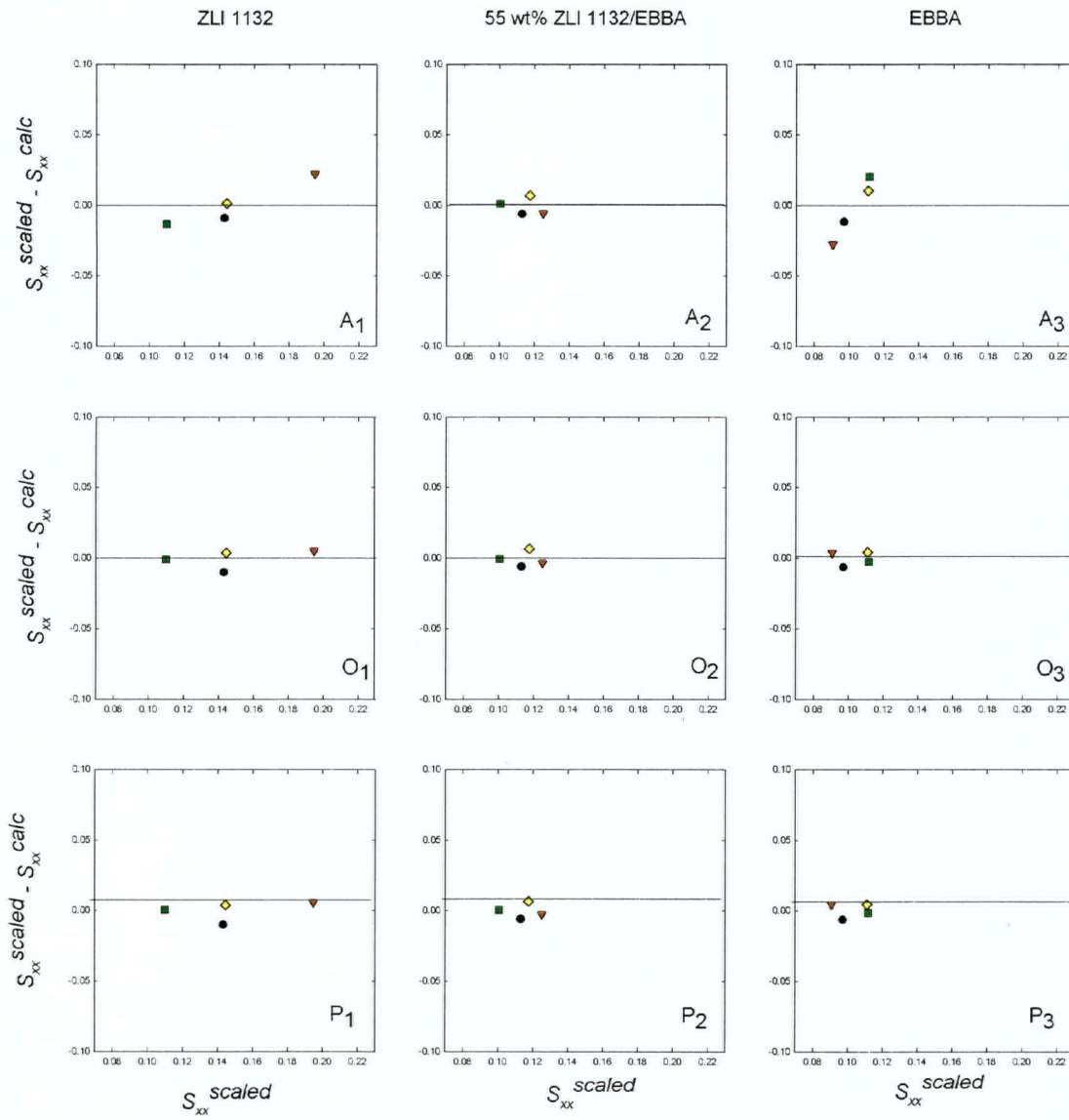


Fig 4.9 Differences between S_{xx}^{scaled} and S_{xx}^{calc} as a function of S_{xx}^{scaled}
 Series A, O and L are results from Fit #1 (CI model), Fit #4 (CI+Polarizability)
 and Fit #6 (CI+Dipole+Polarizability);

● TCB ▼ DCT ■ CLMX ◆ MESIT

4.5 SUMMARY

Short-range interactions are the dominant orientational mechanism in liquid crystal environments. The importance of various electrostatic contributions to the orientational mechanism is still not completely understood. The role of various electrostatic interactions in the orientational mechanism is investigated using small and symmetric molecules with the same size and shape, therefore the same short-range interactions but different electrostatic properties.

According to the RMS and differences in experimental and calculated order parameters of different fits to different combinations of long-range and short-range models, the dipole interaction appears to be least important. On the contrary, results for quadrupole interactions imply that improvement of the fits could be attributed to the effect of the quadrupoles on the orientational mechanism; however, predicted signs of the electric field gradients \overline{F}_{zz} for 1132 and EBBA contradict previous \overline{F}_{zz} study results for component liquid crystals. This interesting observation needs future investigation possibly using the Monte Carlo simulation method.

Single potential fits for all liquid crystals show that the CI model alone accounts the best for the orientational ordering.

In the magic mixture polarizability, alone explains the experimental results better than the other electrostatic interactions alone but still not as good as does the CI model alone. Combined short and long range potential investigations show that in the magic mixture not only is the quadrupole interaction annulled but also the other long-range interactions as well. The polarizability effect appears not to be easily separated from short-range interactions since they both strongly depend on the size and the shape of the molecule. However, examining additive contributions of short-range models with and without the polarizability effect, the polarizability contribution should be considered as an important electrostatic effect in the orientational mechanism.

References:

- [1] Burnell, E. and de Lange, C., 1998, *Chem.Rev.*, **98**, 2359.
- [2] Gelbart, W., 1982, *J.Phys.Chem.*, **86**, 4289.
- [3] Frenkel, D., 1989, *Liq. Crystals*, **5**, 929.
- [4] Vertogen, G. and de Jeu, W., 1989, *Thermotropic Liquid Crystals, Fundamentals*, Springer, Heidelberg, 2nd edition.
- [5] Vroege, G. and Lekkerkerker, H., 1992, *Rep. Prog. Phys.*, **55**, 1241.
- [6] Polson, J. and Burnell, E., 1996, *Mol. Phys.*, **88**, 767.
- [7] Terzis, A., Poon, C., Samulski, E., Luz, Z., Poupko, R., Zimmermann, H., Müller, K., Toriumi, H. and Photinos, D., 1996, *J. Am. Chem. Soc.*, **118**, 2226.
- [8] Terzis, A. and Photinos, D., 1994, *Mol. Phys.*, **83**, 847.
- [9] Photinos, D., Samulski, E. and Toriumi, H., 1990, *J. Phys. Chem.*, **94**, 4694.
- [10] Emsley, J., Palke, W. and Shilstone, G., 1991, *Liquid Crystals*, **9**, 643.
- [11] Photinos, D., Poon, C., Samulski, E. and Toriumi, H., 1992, *J. Phys. Chem.*, **96**, 8176.
- [12] Celebre, G., de Luca, G., Longeri, M. and Ferrarini, A., 1994, *Mol.Phys.*, **83**, 309.
- [13] Syvitski, R., Pau, M. and Burnell, E., 2002, *J. Chem. Phys.*, **117**, 376.
- [14] Gaussian 98, Revision A.9, M. J. Frisch, G. W. Trucks, H. B. Schlegel, G. E. Scuseria, M. A. Robb, J. R. Cheeseman, V. G. Zakrzewski, J. A. Montgomery, Jr., R. E. Stratmann, J. C. Burant, S. Dapprich, J. M. Millam, A. D. Daniels, K. N. Kudin, M. C. Strain, O. Farkas, J. Tomasi, V. Barone, M. Cossi, R. Cammi, B. Mennucci, C. Pomelli, Adamo, S. Clifford, J. Ochterski, G. A. Petersson, P. Y. Ayala, Q. Cui, K. Morokuma, D. K. Malick, A. D. Rabuck, K. Raghavachari, J. B. Foresman, J. Cioslowski, J. V. Ortiz, Baboul, B. B. Stefanov, G. Liu, A. Liashenko, P. Piskorz, I. Komaromi, R. Gomperts, R. L. Martin, D. J. Fox, T. Keith, M. A. Al-Laham, C. Y. Peng, A. Nanayakkara, M. Challacombe, P. M. W. Gill, B. Johnson, W. Chen, M. W. Wong, J. L. Andres, C. Gonzalez, M. Head-Gordon, E. S. Replogle, and J. A. Pople, Gaussian, Inc., Pittsburgh PA, 1998.
- [15] Syvitski, R. and Burnell, E., 1997, *Chem. Phys. Letters*, **281**, 199.
- [16] Patey, G., Burnell, E., Snijders, J. and de Lange, C., 1983, *Chem. Phys. Letters*, **99**, 271.

5. CONCLUSIONS

Extensive comparison analysis of experimental and theoretically calculated order parameters for a series of C_{2v} and D_{3h} type symmetry molecules in a magic mixture support the conclusion that orientation of these solutes is dominated by short-range hard body interactions. In pure liquid crystal components the results suggest that additional long-range interactions might play a role. The dipole interaction appears to be the least important while the quadrupole interaction fits predict different signs of electric field gradient than previous studies [15, 16]. The ambiguity associated with the quadrupole findings should be tested by using computer simulations (MC simulations) as well as checking the validity of statistical approximations employed in the theory.

Finally, the trends among experimental order parameters are the most consistent with the polarizability/short-range model implying that polarizability effects should be taken as an important electrostatic orientational mechanism.